Yeshiva University and Bar-Ilan University Present:

A Collection of Student Research

The YU--BIU Summer Science Research Internship program places select undergraduates in one of the state-of-the-art research laboratories of Bar-Ilan's Life Science or Exact Science Faculties. It enables talented undergraduate science majors to take part in the research of one of Bar-Ilan's more than 180 distinguished faculty members in the biological and/or physical sciences.

Director:

Professor Chaim Sukenik

Av & Em Bayit:

Rav Eliav and Adi

Bar Ilan Professors Involved:

- Ron Adin
- Lior Appelbaum
- Yonatan Aumann
- Mira Barda Saad
- Shay Ben-Arroya
- Ilana Berman-Frank
- Cyrille Cohen
- Haim Cohen
- Aryeh Frimer
- Bilha Fischer
- Sharon Gannot
- Yuval Garini
- Aharon Gedanken
- Doron Gerber
- Ronny Geva
- Eva Gilboa-Schechtman
- Joseph Glicksohn
- Ron Goldstein
- Yoseph Keller
- Osnat Keren
- Lev Khaykovich
- Alon Korngreen
- Moish Koppel
- Sarit Kraus
- Yehuda Lindell
- Rachela Popovtzer
- Malka Schaps
- Amos Sharoni
- Yaron Shav-Tal
- Orit Shefi
- Amelia Somekh-Baruch
- Yossi Steinberger
- Avi Susswein
- Yaakov Tischler
- Zeev Zalevsky

ENGINEERING

Elisheva Aeder (SCW) and Shoshana San Solo (SCW): "Gold Nanoparticles Crossing the Blood Brain Barrier"; Professor Rachela Popovtzer (Engineering).*

In recent years, studies have been conducted showing the benefits of using nanoparticles as passive and active targeting agents as well as contrast agents for molecular imaging. Gold nanoparticles (GNPs), specifically, have been selected for this purpose due to their higher atomic number, resulting in a sharper contrast and decreased radiation dose requirement, and due to their low toxicity, which ensures a higher degree of safety during the imaging process. Linking the GNPs with antibodies, peptides, and other ligands produces active targeting agents which can selectively accumulate on specified cells with receptors for those substances. This process improves precision and accuracy in brain imaging when GNPs are targeted to specific cell receptors, and can allow for drug delivery across the Blood Brain Barrier which protects the brain from external substances.

The blood brain barrier (BBB) is a protective membrane of endothelial cells surrounding the brain with specific receptors that prevent unwanted substances in the blood from penetrating and entering the brain. In order to use GNPs for imaging and drug delivery purposes in the brain, they must be disguised and linked with molecules that will be receptive by the endothelial cells, thus allowing passage of the GNPs through the BBB which would otherwise be impossible. Our project is to test GNPs attached to three different molecules, 2-(4-aminophenyl)benzothiazole (APBT), glucose, and barbiturate, to ascertain which of the three permits the greatest absorption by brain endothelial cells in vitro. These three molecules were chosen: APBT, due to previous verification that compatible receptors exist on the BBB, glucose, because it provides food for the brain and has good transport capacity via transport proteins, and barbiturate which is used for anesthesia and thus is assumed to have receptors on the BBB as well. Barbiturate is also a promising coating option as it improves lipophilicity, a necessary property for crossing the BBB via transcellular lipophilic pathways.

We synthesized GNPs 30 nm in diameter (Figure 1): large enough for efficient detection via imaging modalities and long body retention time, and small enough to permeate cell membranes via receptor-mediated endocytosis. Particles must also be larger than 10 nm because smaller particles are toxic to cells as they can enter nuclei and alter DNA. The particles are prepared using HAuCl4 and sodium citrate. 12-Mercaptodo-decanoic acid (MDDA) is a linker with a thiol molecule on one end that binds with the gold and prevents the particles from aggregating. On the other end there is a carboxyl molecule which is activated by 1-ethyl-3-[3-dimethylaminopropyl]-carbodiimide (EDC) and N-hydroxysuccinimid (NHS), and then conjugated with the desired coating (Figure 2). Additionally, we tested various incubation times of brain endothelial cells injected with GNPs bound with APBT, glucose, and barbiturate to verify the optimum absorption time of the gold into the brain cells. The concentration of gold is determined using a Flame Atomic Absorption Spectrophotometer.

Though it has been previously determined that all three molecules can permeate the blood brain barrier, the purpose of this project is to determine which particles have the fastest penetration and the optimum absorption time, and to eventually test larger particles which can be more easily detected via imaging, and thus can be tracked as they deliver drugs to the brain in a non-invasive way.

In vivo studies are also being conducted in mice to ensure consistency between in vitro and in vivo results. In vivo tests are also necessary to test other molecules such as insulin whose receptors only exist in vivo and not in vitro.

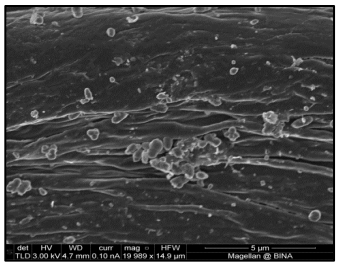

Figure 1: Characterization of GNPs: transmission electron microscopy image of 30 nm GNPs (scale bar 100 nm)

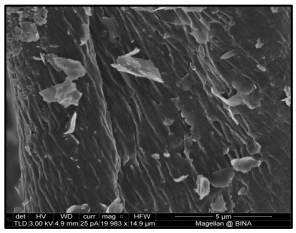

Figure 2: Reactions involving EDC including activation as an NHS ester (taken from thermo scientific online)

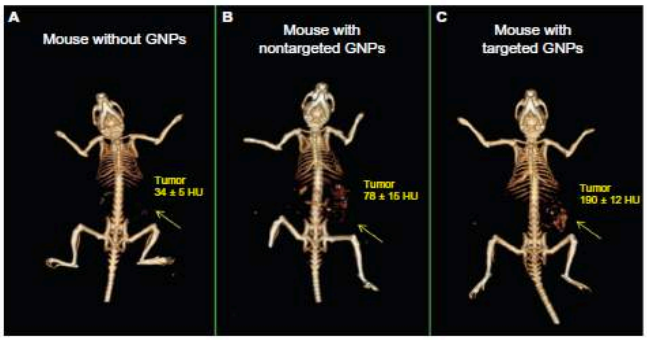

Figure 3: In vivo x-ray computed tomography (CT) volume-rendered images of (A) mouse before injection of gold nanoparticles (B) mouse 6 hours postinjection of nonspecific immunoglobulin GNPs as a passive targeting experiment and (C) mouse 6 hours postinjection of anti-epidermal growth factor receptor (EGFR)-coated GNPs that specifically targeted the squamous cell carcinoma head and neck tumor. The anti-EGFR-targeted GNPs show clear contrast enhancement of the tumor (C, yellow arrow) which was undetectable without the GNPs contrast agents (A, yellow arrow).

*Work done in conjunction with Anat Sharon, Malka Shilo, Menachem Motiei, Dr. Rachela Popovtzer

Judy Alper (SCW): "Neuronal Growth and Regeneration"; Professor Orit Shefi (Engineering).

The nervous system is one of the most pivotal systems in the body in that it determines all other forms and functions. Nevertheless, knowledge of the cellular and molecular mechanisms by which the mammalian nervous system operates, develops, and regenerates still needs thorough investigation. Dr. Orit Shefi's lab attempts to gain a better understanding of how neurons acquire their morphology and use these mechanisms to manipulate neuronal growth. This research has the potential to provide insights which may help enhance neuronal recovery.

I have joined a graduate student, Michal Markus, in a project which tests the effect of iron oxide nano-particles on the neurite outgrowth in rat pheochromocytoma cells (PC12) in the presence of neuron growth factor (NGF). This entailed the seeding of PC12 cells in vitro together with NGF and iron oxide nano-particles. We followed the neurite outgrowth in six different concentrations of nano-particles, from 0 µg/ml (control) to 40 µg/ml, over a period of three days. We analyzed the data collected using the NeuronJ program. The parameters for analysis of the outgrowth included number of neurites from the soma, number of branches, and average total neurite length. Although we expected to see an increase in neurite outgrowth with increased concentrations of nano-particles as well as with time, the results have been inconsistent. The experiment needs to be repeated in order to establish the verifiability of these results.

In addition to measuring neurite outgrowth in vitro, I have joined my lab manager, Dr. Hadas Schori, in a project which involves the analysis of neuronal growth in vivo. To this end, we use a simple model of the nervous system- that of the medicinal leech, Hirudo medicinalis. Inspecting neuronal regeneration in the leech involved dissection, so as to expose, remove, and pin the ganglions. The ganglions, which encase the neurons, can then be subjected to experimentation. We have also attempted to perform leech skin transplantations in order to follow the recovery of the skin and the parallel neuronal contact created. Currently, we are working on setting up the technique for skin transplantation.

Both of the projects discussed have allowed us to gain increased knowledge in both the morphology and function of neuronal development and recovery. The results yielded thus far serve as preliminaries to further examinations and can contribute to uncovering new mechanisms by which neurons can grow and develop.

Akiva Goldstein (YC): "Applying Engineering Principles to Improve Various Processes""; Professor Osnat Keren (Engineering).

The process of transferring information between two points is the basis for almost all forms of technology in the modern world. In order to transfer this information, the data must be processed in a method that would ensure accuracy for the transferred information, which would require the employing of an encoder-decoder system. Constructing the encoder requires combining various MATLAB functions in order to expand the data (given in the form of a polynomial) into the code (which is a larger polynomial). The reason for this expansion is to make it easier for errors in the transference of the information to be found and corrected. The program is designed to take the data polynomial D and the generator polynomial G to create the larger codeword polynomial C through several steps. Firstly, the data polynomial D is multiplied by x^16 in order to create 'I', which is then divided by G in order to find the remainder R. 'I' must be to the power of 255, so if it is smaller than 255, zeros must be added at the end of the polynomial in order to compensate for the difference. The coder is then created through the equation C=I-R.

One of the costliest components of developing a new product i is testing the prototype. There is no one method of testing products, and hence every product test is varied and random, causing each test to become expensive, often times prohibitively so. However, it is possible that there is a way to create a universal test that could be applied for any product, using data gleaned from the way people perceive certain products. Hence, if one were to understand the consumers' general mindset when viewing a product, a single test can be created to cater specifically to the perceptions of the consumer, causing a more streamlined and cheaper trial. In order to discover the perceptions of people, one must ask how they view the workings of a complex yet common system, such as an elevator, in order to understand the different ways a consumer will approach the object, and how he would expect the object to work. This data would be instrumental in the creation of a general algorithm which could be applied to all products to be used for general testing.

Meir Moshe Kurtz (CCNY): "Reliable Data Transmission Rates over Interference Channels"; Professor Anelia Somekh-Baruch (Engineering).

Information Theory is the mathematical theory of data compression, storage, and transmission. Data compression is a method of reducing the space needed to store information and data storage is the storing of data in a way that it can be reliably read at a later time. Data transmission deals with sending information through a channel, usually a noisy channel, without losing any information. One part of data transmission, and the one dealt with in my research this summer, is finding an optimal coding scheme to send messages through a channel.

When a message is sent through a channel, it passes through several stages. First the message must be encoded into a string of characters that can be sent over the channel; for example, turning an email into a binary message that can be sent over the Internet. Next the message must be transmitted over the channel to the recipient and where it is decoded, hopefully successfully. The difficulty in this process arises when the channel, like most real channels, contains noise. In such a case, it is necessary to devise a way to send the message with no loss of information despite of the noise.

A simple and obvious answer to this problem is to send each character in the message multiple times. The most common result would then be assumed to be the transmitted message. For example, if the received message, resulting from the transmission of one character, was 0001101111110, then we would assume that the original message was a 1, that being the more common character. The problem with this method is that to minimize the error, each symbol in the message must be sent many times, causing the rate of transmission to go to zero. This problem seemed impossible to overcome until Claude E. Shannon's 1948 paper. In his paper, Shannon showed that the error in a transmission can actually be made to approach zero while the rate of data transmission approaches a positive number, referred to as the capacity of the channel, if one chooses "good" codewords for the messages. The codewords are assembled into a codebook which is shared with both the sender and receiver. When the receiver receives a signal, he tries to match it to a codeword in the codebook based on the channel characteristics. If the codewords were selected well, exactly one of the codewords in the codebook will correspond to the received signal. The challenge now is to find some "good" coding scheme to make this possible.

In our project, we studied reliable transmission rates for a class of Interference Channels (ICs). An IC is a multiuser channel in which each transmitter has a distinct intended receiver. We compared achievable rates for this channel by writing a program to numerically solve information theoretic optimization problems. To accomplish this, I wrote a program that solves a set of information theoretic equations for every possible probability matrix for a set of multicharacter variables. For a user defined increment, the program recursively generates all possible matrices and for each set, solves the communication problem. The points that define the edge of the region are then plotted in MatLab, with the inner points optionally plotted as well. The plot gives the user an idea of the bounds he faces in terms of transmission rates for each user.

Jonathan Lubat (YC): "Higher Resolution Brillouin Optical-fiber Time-domain Analysis"; Professor Zeev Zalevsky (Engineering).*

The technique called Brillouin Optical-fiber Time-Domain Analysis (BOTDA) is one which allows one to measure the temperature or strain at any point on an optical fiber, from the ends of the fiber. This method is done by using a laser from each end of the fiber, called a pump and a probe. These two lasers interact with each other by Brillouin scattering. We can measure this from the output of the probe on the opposite end of the fiber. The Brillouin scattering is dependent on both the temperature and the strain of the fiber. Therefore, from the output of the fiber, we can tell the Brillouin frequency of every point in the fiber and consequently the temperature and strain at every point in the fiber. Currently, the method either uses a pulse wave for the pump and a continuous wave for the probe, or a pulse wave for both of them. This gives a spatial resolution of a couple of centimeters. However, if we were to use a range of cosine waves for the pump, we would be able to measure a larger output for the pulse. This range of cosines would have many frequencies. Using cosine transforms, we can convert the output to both the time domain and frequency domain to get the Brillouin frequency at a better spatial resolution. This gives us the temperature and strain at every point in the fiber with a higher spatial resolution.

** Worked with Amihai Meiri*

Elli Rappaport (Cooper): "Graphical User Interface for Audio Processing"; Professor Sharon Gannot (Engineering).

Speech has always been considered to be one of the easiest and most useful methods for a user to input commands into any machine. However, for a variety of reasons, speech recognition has yet to meet its true potential and to actually prove useful in day-to-day life. In an effort to improve speech recognition, we have been working on using and comparing different programming libraries and functions to produce a multi-platform graphical user interface (GUI) to view the scope and spectrogram of any audio input in real time along with adjusting its audio output.

We started in MATLAB in order to more quickly and easily produce the different aspects of our GUI before transferring those features to C++ using the QtNokia IDE and libraries. The first step was to analyze different functions for drawing the individual frames of both the scope and the spectrogram plots and deciding at what rate and with which methods the screen should be refreshed in order to give the appearance of a smoothly moving clip. The different methods were compared using the built-in MATLAB Profiler and by paying close attention to the load on the CPU. The remainder of the GUI was then completed to include different features to allow for manipulation and analysis of the graphs, including using mouse input to compare points on the scope. The user is also given the choice to analyze either microphone input or a '.wav' file.

These features were then implemented in C++ using the

QtNokia libraries to communicate with the computer's IO devices. The code uses a series of functions in order to continuously access the contents of both the input and output buffers when available. With a known input sampling rate, the fast Fourier transform (FFT) can be used to calculate the amplitudes of different frequency ranges up until the Nyquist frequency. After breaking down the audio signal into its frequencies, background noise and different voices can be filtered out in order to focus in on the desired speech and analyze only the relevant data.

Elie Weintraub (Cooper): "A Study of Low Pass Filters Using MATLAB and Simulink"; Professor Sharon Gannot (Engineering).

The research conducted had two primary, independent focuses, both of which fall under the general category of signal processing. The first focus was to develop a method of estimating the RC time constant of an RC circuit. The second focus was to successfully implement a fixed-point low pass filter while minimizing the negative effects inherent in quantization.

In order to achieve the first goal, a simple series RC circuit, used here as the most basic of low pass filters, was modeled in Simulink, a platform for simulation and model-based design of dynamic systems. Then two MATLAB programs were developed around this model, the goal of each to estimate the RC time constant of the circuit. Each of the two programs employ parametric fitting—one in the time-domain and the other in the frequency-domain.

In the first program the RC filter takes as input a unit step signal corrupted with random Gaussian noise. The simulation is run several times and the RC time constant of the filter is then estimated by fitting the sets of time-domain filter output data to the analytic equation representing an RC circuit step response. This is achieved using a nonlinear least-squares fit algorithm.

In the second program, the same basic model of the RC filter is employed, this time taking as input a sine wave corrupted with random Gaussian noise. The simulation is run several times with the input sine wave's frequency varying between each run. Then the Fast Fourier Transform (FFT) of both the input signal and the output signal are taken and the composite data derived from the multiple runs are used to compute the frequency response (magnitude and phase) of the filter. The RC time constant is then estimated by fitting the computed, simulation-based frequency response to the analytic frequency response of the RC filter. Again, this is achieved using a non-linear least-squares fit algorithm.

As mentioned above, the second primary focus was to successfully implement a fixed-point low pass filter. As a case study, an input signal composed of two sine waves, one at 2000 Hz and the other at 5000 Hz, was considered. The goal was to filter out the upper tone while preserving the integrity of the lower tone. In order to achieve this goal, first a reference floating-point low pass filter was modeled in Simulink using the MATLAB Filter Design and Analysis (FDA) Tool. The filter was then converted into fixed-point using a 2-step process that made use of both MATLAB's FDA tool and its Fixed Point Tool. In the first stage the word length of the base and accumulator data types were defined. In the second stage the exact Q-format of the different filer components was determined. Different base data type word lengths were explored and the effects of the different levels of quantization were estimated. Additionally, second order section filter decomposition was implemented in order to aid in the mitigation of quantization based error. Finally, the filter's poles and zeros before and after quantization were plotted to ensure that the filter's stability was preserved.

Hillel Weintraub (Cooper): "Developing a Revolutionary Intuitive User Interface Using Shape Recognition"; Professor Yosef Keller (Engineering).

In this day and age interaction with user interfaces (UI's) for controlling machines, systems, and applications has become an integral part of everyday life. To name just two simple examples, television remote controls and standard QWERTY keyboards are a staple of most individuals' daily routines. However, we have identified a number of drawbacks with these traditional interfaces which have provided us with the impetus to design a new type of user interface which can revolutionize the way users interact with end systems. Traditional interfaces vary for each system, and thus, necessitate a time wasting overhead period where the user learns how to use the interface. More importantly, these UI's are not intuitive, frequently containing numerous single function buttons. Finally, many UI's are not accommodating to users whose motion is constrained, such as individuals with motor disorders. We aim to develop a fresh model for user interfaces to combat the above mentioned problems. We will provide a set of shapes that will serve as a universal language or "alphabet" through which users will be able to interact with end systems. It is our belief and hope that the act of drawing and manipulating a small set of shapes will provide a more intuitive and accommodating UI model.

We have chosen to implement our idea on an Android-based tablet with touchscreen capabilities. From a system view perspective, our system can be said to consist of one main block which takes two inputs – a set of preloaded training sample data and a user input shape – and gives one output – a decision as to the identity of the user input shape. The main block implements a shape recognition algorithm to identify the user input shape. We have chosen to make use of shape context descriptors in our algorithm. The idea is that a full image contains a large amount of data, not all of which is useful or necessary. Trying to process all of this data would increase the time complexity of the algorithm to an unreasonable value. We decrease the dimensionality of the data by using the shape context descriptors to encode the relevant shape information from the image and throw out the rest of the data, thus improving the efficiency of our algorithm.

Our development process can be divided into three stages. In the first stage we developed an android application to collect training sample data, and collected samples of the shapes we wanted our algorithm to be able to recognize from multiple users. Next, the raw shape data files were transferred to a PC and used to help optimize our shape recognition algorithm in Matlab. The third stage, which we are currently in the middle of, involves implementing our shape recognition algorithm on the Android platform.

Recently, we have begun work on a new Android application which aims to take our previous work in a different direction, modifying our first system with the goal of creating a tool for the early diagnosis of motor disorders. We hope to be able to exploit distinct characteristics of shapes drawn by individuals with motor disorders in order to identify these individuals at an early stage.

PHYSICS

Malka Sigal

Yoni Mehlman

Paul Creeger

Gilad Barach

Gilad Barach (YC): "DNA Roation Studies Using Tethered Particle Motion"; Professor Yuval Garini* (Physics).

Single-molecule experiments studying the biophysical properties of DNA have revealed many molecular interactions and sub-processes not observable in ensemble studies. An elegant method called Tethered Particle Motion works by conjugating one end of the DNA with a bright particle which can be observed under a microscope. The other edge is fixed to a surface, and the end-to-end distance is easily extracted. Our research group used gold nanobeads (diameter 80 nm) and darkfield microscopy to allow for high image contrast and resolution. Observing how the Brownian motion of the surrounding liquid moved the bright gold nanoparticle allowed for the calculation of the DNA strand's spring constant and persistence length, while the mechanical effect of the presence of specific proteins in the liquid could be easily studied.

The current project involves the use of gold nanorods, one-dimensional sticks of microscopic gold, in place of the spherical nanobeads. Though the added dimension is too small to be directly detected by the microscope, the rod's rotational position can be extrapolated from the microscope's image based on plasmon physics. As extensive study of the optical properties of metals has shown, the polarization of light reflected off of cylindrical shapes depends on the orientation of the incident light, the metal, and the reflection. By gathering data on the DNA's twisting motion in addition to its position, we hope to learn more about how strands of DNA stretch, fold, and twist, both by themselves and in the presence of various enzymes.

*Also under the guidance of Guy Nir and Anat Vivante

Paul Creeger (YC): "Saturation Spectroscopy with Li^7"; Professor Lev Khaykovich (Physics).

Background Atomic transitions are a fundamental characteristics of all atoms and have been measured and calculated many times with much accuracy. Using these previous measurements of the energies of different atomic transitions we can characterize the spectrum of a laser that is causing these transitions as well as other properties of the absorption elements.

Methods Using a homemade external cavity laser (ECL), a single mode narrowband laser was created from a simple diode. Initially, this laser is to enter into a stainless steel vacuum tube with LI-6 and Li-7 inside. The vacuum tube is heated, causing some of the lithium inside to vaporize. Inside the ECL a piezoelectric transducer (PZT) is connected to a function generator, this PZT controls the angle of the diffraction grating thereby controlling the feedback into the cavity and scanning through the frequencies of the ECL. This scanning "probe" beam then passes through the absorption tube, such that if it is at the right frequency it will be absorbed by the atoms inside. Though the laser is narrowband, and it would be expected that only at the proper frequency would absorption take place, the temperature and related velocities of the lithium atoms cause Doppler broadening in the absorption line. Once Doppler broadening is observed, a stronger "pump" laser can be added in the opposite direction through which sub-Doppler lines of specific atomic transitions and their known frequencies may be observed. Once these effects are observed, this relatively weak laser may be locked itself on a specific frequency and in turn be used to lock another more powerful laser (slave laser) to the specific frequencies which are observed in the sub-Doppler.

Results During the experimental work, some minor adjustments to the external cavity were made in order to allow for a better mode-hop-free scanning range of the ECL, as well as changes to the configuration to allow for the most power possible entering the absorption tube. The sub-Doppler and Doppler absorption lines were clearly viewed with improved range and clarity, and on a low resolution spectrometer, as well as on a Fabry-Perot interferometer, injection locking, however was not successfully observed.

Yoni Mehlman (YC): "Noise Measurements in Amorphous Vanadium Oxide Compounds"; Professor Amos Sharoni (Physics).

Crystalline metallic solids have received far more attention from the scientific world compared to their amorphous counterparts. Their orderliness allows scientists not only to study them experimentally but also to quantify their properties and behaviors analytically – to theorize about the physical principles upon which the metals operate. We have decided to study, from a purely experimental perspective, amorphous metallic compounds, particularly Vanadium oxide doped with Niobium. We have observed that the conductivity of certain samples varies greatly with temperature, leading to possible applications for high-sensitivity temperature sensors. However, the effectiveness of a sensor depends on how much electrical noise is present in the system. Unlike the idealized version of current presented in most

basic physics textbooks, actual currents have constant random fluctuations due mainly to heat and external sources. While a properly designed device will minimize external sources of noise, thermal noise and 1/f noise are inherent to any resistive circuit. Thermal noise, which is caused by the motion of electrons due to heat, is directly proportional to resistance and temperature but independent of frequency (white or broadband noise), while 1/f noise depends on the frequency of the signal, being largest at low frequencies. We are exploring two different methods for measuring noise across a wide range of frequencies produced by various amorphous metallic samples in order to determine the relative effects of thermal and 1/f noise as well as to detect any other less common forms of noise. First, we are using a Lock-In Amplifier, a device which measures voltage at a specific frequency, to directly measure the noise at a given frequency by doing a simple frequency sweep on the device. Second, we are using an oscilloscope to measure the oscillations in voltage in the time domain. Then using a fast Fourier transform (FFT) to compute the power spectral density (PSD) we can identify the noise as a function of frequency. We are brainstorming various methods to reduce external noise (which can be quite high in a physics laboratory) and noise produced by the circuit and equipment used for noise measurements. A larger than expected amount of noise has been observed. Further tests are being conducted to determine if this noise is indeed inherent to the metallic sample.

Malka Sigal (SCW): "Directing Neuron Growth: Research from Both ends"; Professor Amos Sharoni* (Physics).

In the course of my research this summer, I examined an experiment from two perspectives: the physical preparatory perspective, and the biological analysis perspective. From the physical perspective, I learned certain techniques to prepare substrates with specific patterns and coatings. After this, the substrates were plated with neurons extracted from the ganglia of leeches, and they were analyzed with a computer program to evaluate their growth.

In Professor Amos Sharoni's lab, I worked with Tal Havdala, one of post-doctorate lab team members. Tal taught me experientially about the process of photolithography. We coated a clean glass substrate with photoresist, a substance whose chemical structure is changed when exposed to ultraviolet light so that it dissolves when placed in a special developer solvent. We used a photolithographic mask to chemically weaken only certain areas of photoresist with ultraviolet light. We then removed those areas of photoresist from the substrate with a developer solvent; this bared a pattern on the substrate that was identical to the pattern on the mask. After this, we sent the substrate to be sputtered. Only the pattern that was exposed to the ultraviolet light was exposed during sputtering. After sputtering, we used a sonicator to remove the excess photoresist still clinging to the substrate, and with it the layer of sputtered material that was not directly touching the substrate. The photolithographic process created a substrate with a certain pattern of sputtered material instead of a smoothly applied sputtering layer across the entire substrate.

Previous research has shown that neuron growth is affected by nanoscale topographic cues such as those that can be produced with photolithography.[1] We are in the process of acquiring a new mask, and when that mask is available, we will move onto the next step in designing substrates with photolithography: using metallic lines instead of non-metallic lines.

This next step required us to see if the neurons will survive on metallic substrates, and if neuron growth on metallic substrates is different from neuron growth on non-metallic substrates. We sputtered different glass substrates with Niobium and Vanadium; we did not use photolithography to create a nano-scale topographic pattern in this new stage of the experiment, since we wanted to test neuron growth on flat metallic substrates as a control before we test neuron growth on metallic lines. At this point, I began to look at the project on neuron growth from the other end, in Professor Orit Shefi's lab, working under Koby Baranes, a Ph.D. student in the lab. Using the ImageJ computer program with the NeuronJ plugin, I traced the neurites extending from each cell to see their length and number. In our analysis of this data, we found that neurons do indeed grow on substrates coated with metals; furthermore, they grow differently than they do on non-coated substrates. When plated on metallic substrates, the neurites tended to branch more often than they did on non-coated substrates, creating shorter average branch length. Further research with neurons plated on substrates with metallic lines created by photolithography will be pursued when the new photolithography mask is acquired.

*Also under the guidance of Professor Orit Shefi, Tal Havdala, and Koby Baranes

[1]Baranes K, Kollmar D, Chejanovsky N, Sharoni A, Shefi O (2012) Interactions of neurons with topographic nano cues affect branching morphology mimicking neuron-neuron interactions. Springer Science+Business Media: author proof

Chemistry

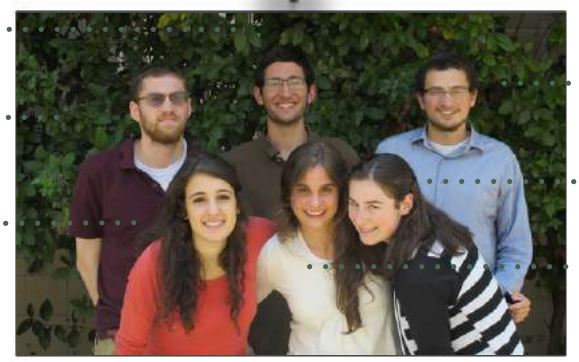

Jacob Cahnman (Illinois): "Coating of Gold Nanoparticles on Glass Substrates using the Sonochemical Method"; Professor Aharon Gedanken (Chemistry).

Gold (Au) nanoparticles were synthesized and coated on glass substrates via sonication as an application in the field of biomaterials to promote neuron regeneration. the general procedure involved sonicating a solution of diluted gold acid (hydrogen tetrachloroaurate) with suspended glass samples, which took place for 30 minutes. The gold nanoparticles formed by redox reaction and high speed jets from the ultrasound forced the particles to bombard into the glass at high speeds, creating strong adhesion to the glass. The glass samples and the solution after the sonication were characterized using SEM and TEM measurements to determine the distribution of the nanoparticle sizes and the location of the nanoparticles on the glass respectively. Polyvinyl pyrrolidone (PVP) was dissolved in the solution prior to sonication and was shown to prevent coalescence of the nanoparticles. It was shown that the best samples were produced when deionized water as opposed to ethanol was chosen as a solvent, when no Polyethylene Glycol (PEG) was used in the solution, and when diluted Hydrazine was added 5-7 minutes after beginning the sonication to act as a reducing agent. After extensive experimentation, it was determined that optimal coatings were produced when 50-100mg of the gold acid was used and 75-150 mg PVP was dissolved into the solution. Neuroblastoma cells were then placed onto the gold-coated surfaces and reacted to slight changes in the nanotopography of the coating. This research has direct applications in creating coatings that can promote nerve regeneration and can potentially help those suffering from nerve damage.

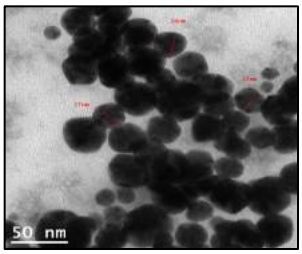

Figure 1: TEM image of the solution of Au nanoparticles demonstrating the distribution of the particle size. Particle diameter ranged from 10-50 nm with an average diameter of 25 nm.

Josh Fluss (YC): "The Synthesis of Receptor Specific Borane-Containing Dinucleotides for Pharmaceutical Research"; Professor Bilha Fischer (Chemistry).

Throughout our bodies, thousands upon thousands of receptors coat many of our proteins. Upon activation, these receptors perform specific functions throughout the body. The goal of medicinal chemistry is to discover and work with some of these defined receptors. This is primarily achieved through modification of compounds which mimic known receptor agonists. The modification can be done to further activate the receptor and increase the function in question, or to antagonize the receptor and thus decrease its function.

Professor Bilha Fischer's lab works primarily with dinucleotides compounds. Not only are nucleotides the "backbone" of DNA, but they also have their own specific purpose, as evidenced by their natural existence in the body. Some specific roles include signal transduction and P2 receptor activation or deactivation.

Through synthesis of dinucleotides composed of a varying number of phosphates in between each nucleotide, Dr. Fisher's lab suggested that compounds containing certain sets of nucleobases and phosphates are more effective P2Y receptor agonists than others, including several previously known natural and synthetic compounds. These compounds became known as the 'lead compound(s)', the start of the work of a medicinal chemist.

Dr. Fisher's group modified the compounds and tested ways in which to improve them. They discovered that by replacing one of the oxygen groups on a phosphate with a Borane group (BH_3), the stability of the compound in vivo was dramatically increased. This proved as one of the most significant steps towards production of a pharmaceutical agent.

This study specifically focused on dinucleotides composed of three or four phosphates, Adenosine and/or Uridine bases, and a Borane substitution either on the α (first) or β (second) phosphate with respect to the from the rightmost base (as shown below).

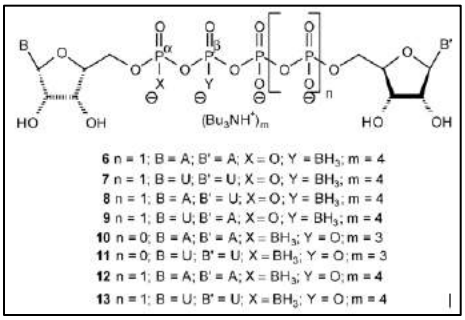

Dinucleoside poly(borano)phosphate analogues synthesized and investigated in the previous study.

By replacing the oxygen of the phosphate with BH_3, the compounds gained an increased resistance to e-NPP1, a natural hydrolysis enzyme. The e-NPP1 breaks down the dinucleotides into nucleotides with one, two, or three phosphates, respectively, and therefore tends to remain in the more metabolically stable forms.

The goal was to find an effective, specific receptor agonist that would be stable in in-vivo living conditions. Several of the dinucleotide combinations were successfully synthesized towards the above goal, and effectively activate P2Y1 and P2Y6 receptors. Dr. Markus van der Giet of Germany will soon begin to study the efficacy of these compounds in activating receptors in animals, specifically receptors that control blood pressure. The ultimate goal is to synthesize a drug which can help treat diseases in clinical trials as well.

My role in this project was to synthesize several of the dinucleotides that seem to be the most promising for future drug development. Reaction conditions require an absence of water. As such, the reactions were conducted using dry vessels and under Nitrogen, preventing an introduction of moisture from the air into the reaction pot. In some cases, the synthesis requires a selective-binding to one of the three hydroxyl (OH) groups. Therefore, the remaining two hydroxyl groups were blocked with a protecting group that would later be easily removed before the yield of the final product. While many of the actual syntheses are simple one-pot reactions, many of the compounds used in the reaction must themselves be synthesized first. Following each step, the compound was purified and tested by Nuclear Magnetic Resonance (NMR) to ensure that the product obtained was the desired product, and to ensure that there were not too many by-products remaining. Finally, throughout this whole process, new solutions must be constantly worked on as the one constant in chemical synthesis is that nothing goes as anticipated

Hudi Jacobson (SCW): "Infrared-Emitting Organic LEDs"; Professor Yaakov Tischler (Chemistry).

Hudi Jacobson[1], Yaakov R. Tischler[2]
1. Stern College for Women
2. Dept. of Chemistry, Bar-Ilan University

Organic Light Emitting Diodes (OLEDs) are part of a new generation of lighting and display technology. They consist of thin layers of organic materials with unique optical and electronic properties sandwiched between two electrodes. These materials can be deposited on numerous substrates and are thus easily stored and carried around[1]. When an OLED is electrically excited, the organic molecules vibrate and their electrons get excited, jumping up to higher energy levels. Eventually, the excitons (excited electrons) relax from their high energy states and fall back to lower levels, emitting radiation.

The cavity in an OLED is comprised of the film of organic material in between the two electrodes. The focus of our experiment was to design the cavity structure for Infrared-Emitting OLEDs by determining which material should be used and how thick the layer should be. An ideal material is one that absorbs and emits in the IR. We test IR absorbance using an FTIR spectrometer (see Figure 1).

Figure 1: BRUKER FTIR specrometer used in our analysis

We spin-casted thin films of Polystyrene and Polymethyl Methacrylate with varying concentrations in order to achieve a thickness similar to the size of a wavelength of infrared light. The data showed that Polystyrene displayed good absorbance peaks in the IR at wavenumbers which are multiples of 700 cm^{-1} (see Figure 2), similar to what we found in the literature[2]. We therefore decided to work with Polystyrene and to concentrate on making a film that was thick enough for our cavity.

We made several solutions of Polystyrene in Chloroform and constructed a spin curve (see Figure 3) to decide which speed and which concentration yield a film that of optimal thickness for our experiment.

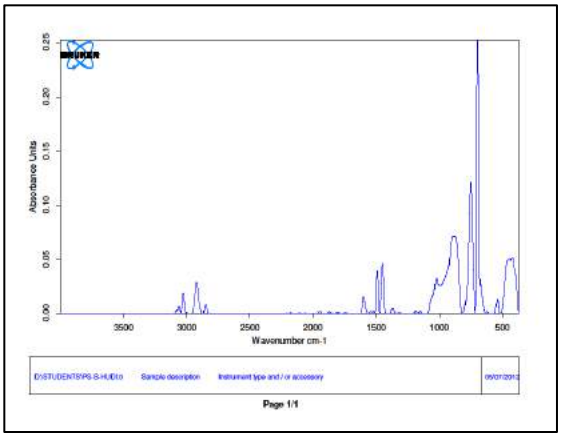

Figure 2: FTIR absorbance curve for Polystyrene

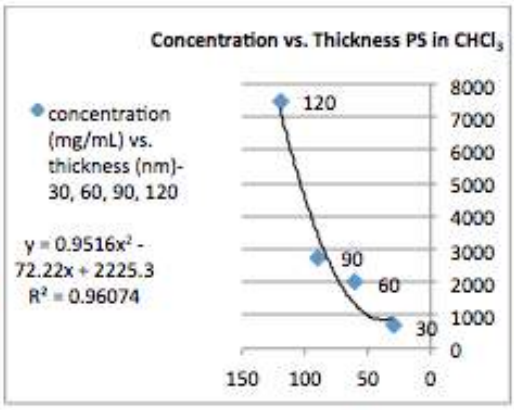

Figure 3: Spin curve for various concentrations of Polystyrene in Chloroform

The ideal film thickness was determined to be approximately 4.6 microns, based on Bragg's Law $d=\lambda/2n$, where d is the film thickness and n is the index of refraction of our material.

Current work involves constructing diodes using Potassium Bromide as a substrate, since this material is almost completely transparent in the IR wavelength range of interest. Our diode will be composed of a round disk of KBr, two 20 nm-thick silver electrodes and an optimally thick organic layer of Polystyrene spin-casted from Chloroform with a ratio of 105mg/mL. We plan to test the IR emission of the diodes using a SPEX 270M monochromator and an IR detector.

Eventually, we hope to use this model to create inexpensive IR-emitting OLEDs which can be used for chemical sensing, as well as in solid state IR lasers.

Sarah Mizrachi (SCW): "Antibacterial Properties of In Situ Generated and Simultaneously Deposited Nanocrystalline Zinc Oxide, Magnesium Oxide, and Calcium Oxide on Fabrics" Professor Aharon Gedanken (Chemistry).

Sarah Mizrachi[1], Aharon Gedanken[2], Nina Perkas[2], Ilana Perelshtein[2]
[1] Department of Physics, Stern College for Women, Yeshiva University, New York, NY
[2] Department of Chemistry, Bar-Ilan University, Ramat Gan, Israel

The coating of fabrics with certain types of nanocrystals can impart the fabrics with resistance to bacteria. This research has many potential applications, especially in hospitals. A material's resistance to bacteria can be maintained without the medical problems induced by systemic antibiotic administration, such as immune suppression and micro-organisms forming resistance. In these experiments, Zinc Oxide, Magnesium Oxide, and Calcium Oxide nanocrystal combinations were synthesized and distributed onto cotton fabrics to impart them with antibacterial properties.

Ultrasound irradiation is a technique used to stimulate the formation of nanoparticles and their application onto a substrate. The effect of sonication comes from the cavitation process that involves bubble formation, growth, and collapse, producing high energy microjets. This process stimulates the formation of anti-bacterial nanoparticles and homogenous coating of the fabric. The nanocrystals, reacting from combinations of Zn-acetate, Mg-acetate, and Ca-acetate, were formed in situ and deposited onto a cotton fabric bandage. Techniques, including X-ray Diffraction, Scanning Electron Microscopy, and Inductively Coupled Plasma (ICP) Analysis, were then applied to better understand the crystal structure of the nanoparticles that formed.

The Scanning Electron Microscope images below show how the ZnO nanoparticles were found to be more round in nature, and better embedded into the fabric than the nanoparticles containing both ZnO and MgO.

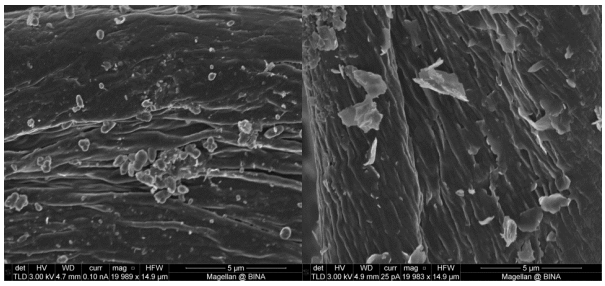

Scanning Electron Microscope Images of ZnO-Coated Fabric (Left) and ZnO/MgO-Coated Fabric (Right)

The anti-bacterial properties of fabrics coated with various combinations, ratios, and concentrations of ZnO, MgO, and CaO were then measured and analyzed. The fabrics were tested against both Gram-negative and Gram-positive bacteria. The nanoparticles were found to generate free radicals and hydroxyls that damage bacterial cells when coming in contact with them. Antibacterial tests on the samples are still in progress, and conclusions regarding which combinations, ratios, and concentrations of these nanocrystals have the greatest antibacterial properties can impact the future of antibacterial nanotechnology.

Debra Rosenbaum (Barnard): "Locating Intercalants within Synthetic and biological Membranes"; Professor Aryeh Frimer (Chemistry).

The cell membrane plays a critical role in protecting the cell from potential pathological agents by modulating the crossing of chemicals into and out of the cell. This modulation is determined based on the interaction between the particular chemical and the polarity gradient of the membrane, as determined by the skeletal molecular structure of the phospholipid as well as the complex system of functionalized proteins, phospholipids, and cholesterol lodged in its bilayer.

Professor Aryeh Frimer's lab studies the hydrophobic phospholipid bilayer of the dimyristoylphosphatidylcholine (DMPC) liposome in an effort to understand the more highly functionalized biological membrane. The hydrophobic bilayers have a unique chemistry that occurs within them. The lab focuses on the interaction between toxic, highly reactive oxygen radicals—

particularly the superoxide anion radical ($O^{\cdot-}_2$), —with the hydrophobic regions of the biological membrane. Specifically, the research objective is to understand the extent to which the superoxide anion radical penetrates the bilayer as a result of its chemical and biological reactivity. Once these interactions are understood, it may facilitate further understanding of the role oxygen radicals play in the aging process, cancer, multiple sclerosis, Parkinson's disease and senile dementia.

The embedded substrates of the biological membrane allow for a fluid structure, and the compositional phospholipids vary in chain length. As such, measured location of a substrate can only be qualitative. The liposome model is therefore used, as it has a more rigid structure with consistent phospholipid chain lengths, and can allow for a quantitative measure of the location of the embedded substrates.

In order to more precisely understand the reactions of the superoxide anion radical, the depth and orientation of substrates, as reacted with the superoxide radical anion, needs to be determined. The intercalation of these substrates within the biological membrane was monitored using the NMR technique, allowing for the expression of the location of these molecules in terms of a polarity scale, based on Reichardt's $E_T(30)$ parameter. Once the location of these molecules is determined, it may be possible to define which derivatives successfully intercalated into the membrane. This information will then allow us to construct a partial chemical ruler which may permit eventual determination of the intercalants within the liposomal bilayer in Å values. We can then attempt to understand the relationship between the location of the substrate in the liposomal hydrophobic bilayer and its chemical and biological reactivity. Fatty-acid derivatives, each with a ketone moiety on varying carbons (n= 4, 6, 8, 10, 12) along the alkyl chain, were synthetically prepared and monitored by NMR. These fatty-acids (keto-phospholipid) [fig. 1] were then attached to a phospholipid head group, with the ketone carbonyl serving as the variable marker, and subsequently intercalated into the bilayers of the DMPC liposome dispersed in aqueous media (via sonication or vortex).

A correlational graph was constructed, measuring the chemical shifts [in ppm] against polarity [Reichardt's E_T (30) parameter], through use of the NMR method. Because there exists a polarity gradient in the bilayer, the intercalated molecules feel a different polarity based on their environment, and thus the carbonyl location [measured in E_T (30) parameter] from the water-lipid interface was determined.

Comparison of the intercalated synthesized molecules (keto-phospholipids) of different carbon derivatives to a pre-prepared correlation graph of the various polarizable carbons of a substrate with known $E_T(30)$ values allowed for successful construction of the "chemical ruler" [fig. 2].

The chemical ruler, as based on the DMPC model can be compared to the intercalated molecules into the biological membrane. The plentiful and cost-efficient erythrocyte ghosts (isolated membranes of Red Blood Cells) were used as this biological membrane, and were combined with the synthesized DMPC liposome. NMR spectra conditions were optimized, allowing for identification of the intercalated phospholipids [Fig. 2].

Results obtained thus far indicate that less lipophilic/ hydrophobic compounds do not intercalate within the bilayer; moderately lipophilic/ hydrophobic compounds intercalate close to the head group region of the biological membrane; and the very lipophilic/hydrophobic molecules intercalate deeply into the bilayer.

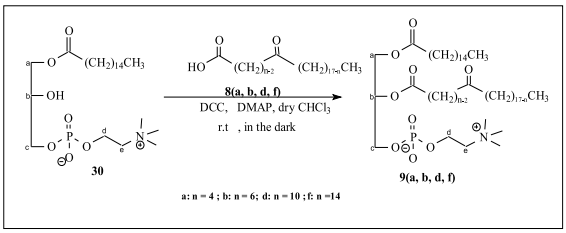

Figure 1: General synthesis to obtain the fatty acid (keto-phospholipid)

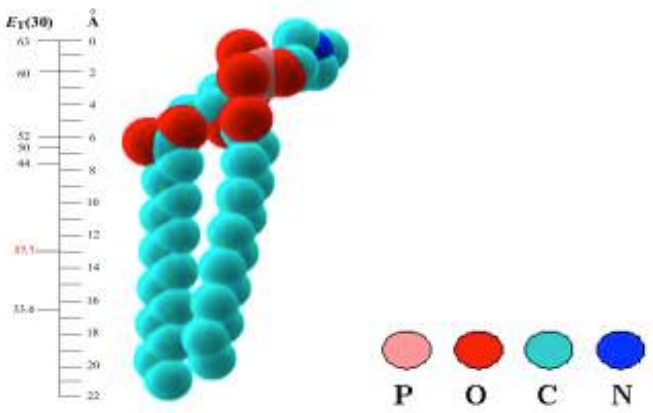

Figure 2: Improved Chemical Ruler

Efram Stone (YC): "Pulp Probe Spectrometry and Monochrometer Capatibility"; Professor Yaakov Tischler (Chemistry).

General Information:

Pump probe spectrometry is a method of measuring transient changes in the absorption of a material that has absorbed a separate light pulse within the last few picoseconds. In order to accomplish this, we send a "pump" light pulse through a material, followed shortly by a "probe" light pulse. A chopper shuts off alternate pump pulses, giving us a base absorption pattern that can be subtracted out. A stage with mirrors changes the distance that the pump pulse has to travel, which in turn changes the time between the arrival of the pump and probe pulses. The pump pulse then travels through a spectrometer, where it is separated into its component wavelengths by a grating. Moving this grating controls which wavelengths reach the exit. We can also control whether a camera or a photo-detector takes the readings. The photo detector can only record one wavelength at a time, whereas the camera can record all of them, but the camera is normally much too slow for this application, and

some tricks must be used to reach a sufficient speed. All programming was done in labview.

Single delay pump probe:

I updated an existing pump probe program that had only controlled the stage so that it also controlled the spectrometer, removing the necessity of doing things like opening the shutter manually. To the existing functionality of checking a series of delays at a given wavelength, I added an option of checking a series of wavelengths at a given delay. Because this program uses a photo-detector, it can only check one point at a time, so checking absorbance for multiple delays and multiple wavelengths would take an impractically long time, especially in a lab where other people need to use the spectrometer.

Shifting registers(custom chip) and the CCD array:

In order to use the camera, we need to update the speed at which the CCD(the part of the camera that takes pictures) records data. We can accomplish this using the camera's custom chip settings. These allow the camera to take a picture with part of the CCD, move the picture to an inactive part of the CCD, and repeat. This can be repeated several times, and allows the CCD to accomplish the time–consuming task of actually reading data from the array after the readings have been taken, and is also known as shifting the registers because of the way that the data in the registers is shifted without being read. I modified the single wavelength program above so that it can do this, but did not complete bug fixing.

Compatibility of a Spex 270m imaging monochrometer:

In addition to the above programming, I attempted to interface an old spex 270 imaging monochrometer and a lock-in amplifier with a computer, so that Judith Jacobson can use it to measure spectral emission lines in the infrared. After around two and a half weeks of work, I managed to get the monochrometer, but not the lock in amplifier, to work with the Winspec spectrometry program.

Math & Computer Science

Aviva Bukiet (NYU): "Fitting the Smile"; Professor Malka Schaps" (Math).

My research this summer dealt with analyzing the cost of stock options. An option is an agreement between two parties to allow for a transaction by a specified future date around a predetermined price known as the strike. There are two different types of options: calls and puts. The buyer of the call option pays to gain the right but not the obligation to buy an agreed quantity of a particular commodity at the strike price before the option expires. The buyer of the put option pays a price to gain the right to sell an agreed upon quantity of a particular commodity at the strike price before the option expires. Based on the strike price, the volatility of the stock, and the time until the option expires among are just some of the variables used determine the price of the option. Using various complex formulas, I worked to develop a program that predicts whether the stock option is priced too high or too low. The program graphs the pricings of the options alongside an artificial curve that we created that predicts what the pricing should be from a mathematical view. The graph comes out to look like a smile and is thus named "The Smile Curve." If there is a large variation between any point and the curve, then we would recommend you take relevant action in the market.

Tzvi Goldfeder (YC): "Implementing Yao's Garbled Circuit" Professor Yehuda Lindell (Computers).

The problem of Privacy-Preserving Data Mining arises when two parties have data sets that they do not want to or cannot share with each other, but they want to compute a function on the joint data set. A simple example involves finding the intersection of two sets. Person A has a set of numbers as does Person B. They want to find the intersection of their sets while maintaining their respective privacy. Privacy in this context means that nothing can be learned from the computation more than that which can be derived from the output directly. So, in our example, while the intersection itself (i.e. the output) will tell each party some information about the other party's set, nothing additional should be learned from the computation.

Yao's protocol provides a general method for Privacy-Preserving Data Mining. The protocol first requires that the function to be computed be expressed as a combinatorial circuit. This is a fair requirement for any polynomial-time function can be expressed as a combinatorial circuit of polynomial size (see Secure Multiparty Computation for Privacy-Preserving Data Mining by Lindell and Pinkas). The parties will agree upon a circuit to solve their problem. One party will take this circuit and from it compute a "garbled circuit". The garbled circuit will be topologically identical to the ungarbled circuit. The difference is in the values on the wires. Whereas the regular circuit's wire's value is either 0 or 1, the wires of the garbled circuit are assigned a garbled value. Each wire can assume one of two possible garbled values corresponding to 0 and 1. However, the important thing is that the actual {0,1} value cannot be learned from the garbled value.

Now, assume that a gate contains two input wires. The gate will have four values corresponding to the four combinations that the values of these wires can contain (there are two wires each of which can assume one of two values). Each of the four values at the gate is a double encrypted garbled value. The values of the two input wires are keys to decrypt one and only one of these values at the gate. (Actually, as we will see below, it is possible that more than one of these strings can be decrypted but only one of them will be the "correct" decryption that we are looking for.) The party evaluating the circuit will use these two keys to decrypt the value, and the result will be the garbled value of the output wire.

The process of evaluating the values of the gate will continue until the entire circuit has been evaluated and the computing has obtained garbled output values. A separate function will then translate the garbled output into meaningful output using a translation table provided by the party that constructed the circuit.

Having discussed how the circuit is computed, the remaining issue is putting in the input values privately. The party that constructed the circuit can just pass along the garbled value of its input to the evaluating party. Since the values are garbled, the evaluating party does not learn anything about the actual values and privacy is maintained. The difficult part though is how the party that is evaluating the circuit will obtain its input values. It cannot ask for the value that it wants (i.e. "Give me the garbled value encoding 0 on wire 1") since that will reveal its input to the other party. Also, the constructing party cannot just hand over both values, since that will allow the evaluating party to learn more about the circuit than it should be allowed to (i.e. it will be able to

learn more than can be learned from the output itself). We need a method that will allow the evaluating party to learn the garbled value of its input only, while the constructing party learns nothing. To achieve this, we use a 1-out-of-2 oblivious transfer protocol that accomplishes just this. Using oblivious transfer, the evaluating party learns only the value of its input and the constructing party learns nothing—i.e. it does not know whether the other party received the 0-value or the 1-value. (There are different oblivious transfer protocols depending on the type of adversary.)

It is important to differentiate between a "semi-honest" and a "malicious" adversary. A semi-honest adversary is one that follows the protocol, but may try to learn more from the transcript of the message that it received. Thus, with a semi-honest adversary, we need only to ensure that assuming it follows the protocol, it does not obtain any information that it should not have. A malicious adversary, on the other hand is not assumed to follow the protocol. The protocol that we have described so far holds for a semi-honest adversary only. For a malicious adversary we must (1) use an oblivious transfer protocol that is secure for malicious adversaries, and we must (2) ensure that the party is constructing the circuit correctly (i.e. that the garbled circuit is identical to the agreed upon circuit). To ensure that the party is computing the circuit directly, a variant of Yao's protocol calls for the constructing party to construct multiple copies of the circuit. The other party will then choose which one it wants to use for computation and which ones it wants to inspect. It chooses the ones that it wants to inspect and asks the constructing party for both garbled values (keys) on each input wire. It then works its way through the circuit by using these values to test that the gate is computing the correct function (e.g. to test that a gate that is supposed to be an AND gate is indeed an AND gate). In the process of testing each gate, it obtains both garbled values for the output wire of that gate and can then test the next gate. It continues this process until it verifies the correctness of every gate in the circuit. Once it inspects these circuits and finds them to be correct, the probability is high that the circuit that it is actually using to evaluate is also constructed correctly. This summer, I implemented the non-communicative aspect of Yao's protocol in Java. I created a program that creates and computes garbled circuits and also verifies that they have been constructed correctly. I used modular design so that the software can easily be customized with any encryption scheme. The gates can be garbled using any CPA-secure encryption scheme as well as any other form of encryption. One non-traditional garbling scheme that I implemented uses collision-resistant hashing for its encryption. Additionally, I designed the software so that circuits can be created and computed in parts, reducing the memory requirements as there is never a need to store an entire large circuit in memory.

Yosef Hoffman (YC): "Cake Cutting: Bounding the Maximum Degradation of Social Welfare Due to Fairness Criteria in Chore Division Scenarios"; Professor Yonatan Aumann (Computers).

Introduction. The classic "cake-cutting" problem is as follows: There are n players who intend on fairly dividing a "cake" amongst themselves. Each of these players has his/her own valuation of which parts of the cake he/she prefers. The goal is to create a division that maximizes social welfare, while taking into account fairness requirements. We aim to provide bounds on the maximum sacrifice of social welfare caused by these fairness constraints. Previous works have dealt with the division of goods, where players have a utility function and like parts of the "cake." Here, we focus on the division of chores, where players have disutility functions and dislike parts of the "cake." Although these scenarios are similar, many of the ratios and proofs that hold true for goods fall apart when dealing with chores. We consider cases with an additional requirement that each player receives one contiguous piece. Other works have investigated cases in which players can receive any number of pieces from anywhere in the cake, but to our knowledge no one has yet looked at cases with this constraint.

Fairness Criteria. It is important to look at social welfare when trying to decide how to split up a cake. After all, we want to maximize the total happiness. But there is also an aspect of fairness to each individual player. We consider the three major fairness requirements:

- Proportionality – each player gets at most 1/n of the cake (by his/her own valuation)
- Envy-Freeness – no player prefers getting the piece allotted to any of the other players
- Equitability – all of the players get the exact same disutility (by their own valuations)

Social Welfare Functions. There are also different ways of assessing social welfare. The utilitarian social welfare is the total disutility of all of the players combined. Maximizing this type of welfare ensures that we have the most happiness overall, but it may sacrifice the happiness of individuals. Egalitarian social welfare addresses this issue by only taking into account the disutility of the player who is worst off. We consider these two types of social welfare functions.

Price of Fairness. In order to quantify the degradation of social welfare due to the different fairness requirements, we define the notion of Price of Fairness, in its three forms – Price of Proportionality, Price of Envy-freeness and Price of Equitability, defined as follows. The Price of Proportionality (resp. Envy-Freeness, resp. Equitability) of a cake-cutting instance I, with respect to some social welfare function, is defined as the ratio between the minimum disutility attainable when divisions must be proportional (resp. envy-free, resp. equitable) and the minimum possible disutility for the instance, taken over all possible divisions. For example, if $X_{EF} \subseteq X$ is the set of all (connected) envy-free divisions of an instance, the egalitarian Price of Envy-Freeness for this instance is

$$\frac{min_{y \in X_{EF}}\, eg(y)}{min_{x \in X}\, eg(x)}$$

Results. We aim to show bounds on the maximum utilitarian and egalitarian Prices of Proportionality, Envy-Freeness and Equitability of any instance. Our results for chores, along with the previous results for goods, are summarized in Table 1, where n is the number of players. An upper bound means that the respective price of fairness of any instance in the class is never greater than the bound; a lower bound means that there exists an example of an instance with at least this price of fairness. A bound is tight when the lower bound exactly matches the upper bound.

Price of:	Proportionality	Envy-Freeness	Equitability	
Utilitarian	n	∞	n	Chores (this work)
Egalitarian	1	∞	1	
Utilitarian	UB: $\frac{\sqrt{n}}{2}+1-o(1)$ LB: $\frac{\sqrt{n}}{2}$		UB: n LB: $n-1+\frac{1}{n}$	Goods (previous work)
Egalitarian	1	$\frac{n}{2}$	1	

Table 1: All Results

We provide a tight bound of n on the utilitarian Prices of Proportionality and Equitability. We show that the Price of Envy-Freeness, using either the utilitarian or the egalitarian social welfare function, is unbounded (for n>3), meaning that there is no maximum amount of social welfare that may have to be forfeited for the sake of envy-freeness. Additionally, we demonstrate that the egalitarian Prices of Proportionality and Equitability are 1, which means that no amount of social welfare is lost for the sake of proportionality or equitability.

Baruch Lane (CUNY): "Automated Human Persuasion by Artificial Intelligence Agents" Professor Sarit Kraus (Computers).

I am conducting research in Artificial Intelligence by programming experiments in automated human persuasion by AI agents.

Professor Sarit Kraus's multi-agent systems laboratory at Bar Ilan University specializes in the interactions between multiple automated agents, as well as the interactions between automated agents and humans. The part of the laboratory that is dealing with human-agent interactions is working to implement machine-learning techniques to improve automated agents' abilities to understand and interact with humans.

I am working with Maier Fenster, a doctoral student in the laboratory. The goal is to influence humans' decisions using an automated agent. In our current experiment we show images to a subject and the subject needs to choose a point of interest in the image. The automated agent controls the context of the experiment in an effort to manipulate the subject's interpretation of the images. We assess the manipulation by measuring the changes in the probability of the subject selecting a given point in an image.

Much of my work has been focused on developing software to be used in the experiment. So far I have finished programming the run-time module for the first stage of the experiment. I have also nearly completed software used to set-up the experiment. I will shortly be programming software for result presentation. The run-time module was implemented as a platform-independent client with a very light-weight server. I also integrated the module with Amazon Mechanical Turk which we use to find and compensate subjects of the experiment.

We have completed the initial stage of the experiment and have begun testing on multiple subjects. In future stages we intend to optimize the machine learning algorithm that controls the context of the experiment in an effort to improve the automated agent's ability to interact with human subjects.

Toviah Moldwin (YC): "Machine Learning Methods for Authorship classification Queries"; Professor Professor Moish Koppel (Computers).

The problem of identifying various things about the author of a text, whether it is the author's identity, personality, or political affiliation, is a question which frequently becomes important in the study of humanities. Author identification is an especially relevant topic for the study of Jewish religious texts, many of which are written anonymously, pseudonymously, or by multiple authors. There are a number of subsets of the authorship attribution problem: discerning whether a document was written by author A or author B, determining which of a large set of authors wrote a particular text, or verifying whether an individual is or is not the author of a document.

While a variety of techniques have been used in the past to resolve queries about authorship, modern machine learning techniques can help answer these questions in a more rigorous fashion. Machine learning algorithms traditionally used to categorize documents based on content can be modified to extract information about a text's author. Whereas content classification generally uses content words to classify texts, authorship attribution models use features that are likely to be endemic to a particular author, time period, or personality type. Some of the most significant feature types for authorship identification include function word frequency, n-gram frequency, and grammatical morphology. Models with these features can be constructed from training sets for which the classification is already known, and query texts can then be classified based on their similarity to the models created from the training sets.

The relative similarity of two texts can be determined in a number of ways. One approach is to model texts as points or vectors in n-dimensional space. Each dimension of the space represents a feature, and a document's normalized value for the frequency of each feature determines the position of the point or vector representing the document within the space. Various geometric techniques, such as Euclidean distance and cosine distance, are then used to determine the similarity of documents to each model. Other methods, such as naïve Bayes classification and support vector machine (SVM), can also be used to create models and classify documents.

The reliability of a particular set of features for creating an accurate classification model can be ascertained either by testing the model on already-classified documents or by performing K-fold verification, wherein the training texts are divided into K parts, K-1 of which are used to create a model and 1 of which is used as a query set. This process is repeated K times, each iteration using a different part of the training corpus as the query set. The accuracy and recall of the K-fold verification helps predict how accurately the algorithm will be able to classify a query text whose classification is currently unknown. The accuracy and recall that can be obtained via machine learning vary greatly depending on the particular training sets and the difficulty of the query, but machine learning remains one of the best tools at our disposal to

resolve questions of authorship classification.

For the purposes of running multiple classification experiments on a known corpus of texts, a user interface is needed to aid the selection of classes, relevant features, query texts, and classification methods. In addition to working on the back-end code for the classification algorithms, I have been developing such a graphical interface that will make these machine learning algorithms accessible to humanities scholars who don't necessarily have a background in machine learning techniques. With the aid of this interface, humanities scholars should be able to solve (or at least come much closer to solving) age-old document classification problems in a matter of seconds, instead of spending months – if not years – studying the texts with human insight alone.

Eliezer Snow (YC): "Enumeration of standard Young tableaux of certain truncated shapes, continued"; Professor Ron Adin (Math).

A standard Young tableau (SYT) consists of a table with n boxes, each filled with one of the numbers between 1 and n such that numbers increase along both rows and columns (see figure 1). Standard Young tableaux have numerous applications in combinatorics, representation theory, and algebraic geometry. As an example, it can be shown that the number of SYT on a given standard shape of size n is equivalent to the dimension of a related representation of Sn [3]. An SYT is said to be in a standard shape if the shape is aligned on the left and row length is weakly decreasing (less than or equal to the previous row) from top to bottom (see figures 2 and 3). In such a scenario, there exists a well-known "hook-length formula" to enumerate all possible SYT of a given shape ([2], [p. 214]). When a standard shape is truncated, however, no general formula is known.

In [1], Adin and Roichman began exploring specific truncated shapes, such as squares and rectangles with one or two boxes removed from the northeastern corner (figure 4). Similar studies were carried out by Panova [4]. We continued this project by researching conjectured formulas for shapes of the form (n^2) \ (n – 2), (figure 5), (n^2) \ (n – 3), (figure 6), and n(n + 1) \ (n – 2) (figure 7). In addition, we sought to understand in which scenarios we could expect a product formula, and in which scenarios no such formula exists.

To discover a conjectured formula, Adin and Roichman developed a bijection between a large truncated shape and a combination of two smaller standard shapes. This allows us to count the number of standard Young tableaux (NSYT) by counting all the possible combinations of smaller shapes in the range of the bijection via the already known hook-length formula. If NSYT consistently contains only relatively small prime factors (at most the size of the shape), this indicates the existence of a product formula.

After applying this method to the shapes mentioned above, we obtained positive results for those shapes with a first row of length 2, and negative results for shapes with a first row of length 3. We conjecture that for n > 7, the largest prime factor of NSYT for the shape (n^2) \ (n -2) is the largest prime number less than n^2. We further conjecture a generalized formula for any shape of the form of a k by n rectangle with a row of two squares appended to its NW corner to be (F(k) F(n) (kn-k)! (kn+n)!) / (F(n +k) (kn+n-k)!), where k is the number of rows (excluding the appended row of length 2), n is the number of columns, and F(m) is defined as the product of the factorials of x for x in range(1, m). This formula has been proven analytically for k = 2,3, and verified computationally for all rectangles between the sizes of 2 by 2 and 20 by 20.

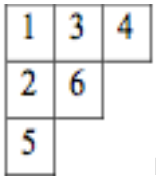

Figure 1: A Standard young tableau

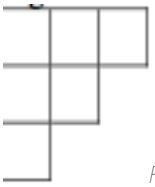

Figure 2: A standard shape

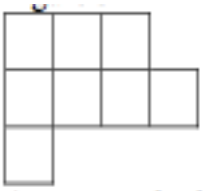

Figure 3: A non-standard shape (row 2 is greater in length than row 1

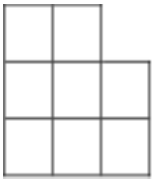

Figure 4: A truncated square shape, with one box removed from the NE corner

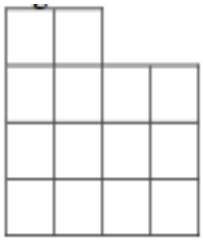

Figure 5: The shape (n^2) (n-2) for n = 4

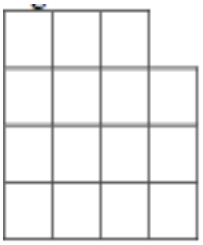

Figure 6: The shape (n^2) / (n-3) for n = 4

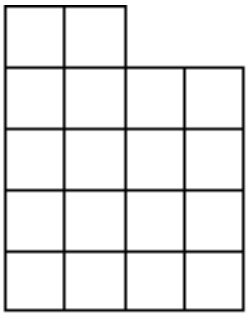

Figure 7: The shape(n(n+1))/(n-2) for n= 4*

Acknowledgements:

Thanks to both Yeshiva University and Bar-Ilan University for their generous support of the summer research program at BIU. We are extremely grateful to Professor Chaim Sukenik for the hard work he puts in to make this program a success. Last but not least, many thanks to Professors Ron Adin and Yuval Roichman, from the Department of Mathematics at Bar-Ilan University, who gave extensive guidance to the author on this project.

References:

[1] R. M. Adin and Y. Roichman, Enumeration of Standard Young Tableaux of Certain Truncated Shapes, Electron. J. Combin. 18 (2011), no. 2, Paper 20, 14 pp.

[2] M. Bona, Combinatorics of Permutations, Chapman & Hall/CRC, Florida, 2004.

[3] W. Fulton, Young Tableaux, with Applications to Representation Theory and Geometry. Cambridge University Press, 1997.

[4] G. Panova, Tableaux and Plane Partitions of Truncated Shapes, Advances in Applied Mathematics, In Press, Corrected Proof, Available online 13 June 2012.

[5] B. E. Sagan, The Symmetric Group. Springer, New York, 2001.

[6] D. Wagner, Understanding Representation Theory and Tensor Products via Young Tableaux, Math Honors Thesis, Hillsdale College, May 2009.

Nathan Japhet
Steven Krausz
Shira Redlich
Michaela Gasner
Miriam Steinberger
Mordechai Smith
Avi Bursky- Tammum
Shalom Benzaquen
Dahlia Pasik
Sarina Miller
Aliza Loshinsky

Shalom Benzaquen (U Ottawa): "Aging and a Protein That Affects It"; Professor Haim Cohen (Life Sciences).

Within the past century, the extension of lifespan in humans due to technological advances in the medical field have brought with it novel age-related metabolic diseases. The most prevalent of these is metabolic syndrome, which affects an estimated 25% of the US population. Metabolic syndrome includes a number of disorders including abdominal obesity, dyslipidemia, glucose intolerance, insulin resistance, and premature appearance of age-related diseases, such as diabetes type II, hypertension, generalized inflammation, and a propensity towards developing neurodegenerative diseases (Grundy et al., 2005; Milionis et al., 2008; Huang, 2009). Further research must be conducted to determine the connection between metabolism and aging.

It has become widely known that a calorie restricted (CR) diet slows the rate of aging and extends the lifespan of many organisms, including yeast and rodents (McCay et al., 1935); (Weindruch & Walford, 1988). It has been shown that rodents fed a CR diet show many of the phenotypes that are the direct opposite of the metabolic syndrome, including decreased total body fat, LDL-cholesterol, free fatty acids (FFA) and triglycerides, improved glucose tolerance, and increased HDL-cholesterol. Additionally, research has shown the CR diet delays the appearance of many age-related disorders such as cancer, diabetes, and neurodegenerative diseases (Weindruch & Walford, 1988; Fontana & Klein, 2007). Thus, it is possible that metabolic syndrome and CR-associated changes life at diametric ends of the same spectrum and involves an overlapping set of regulators (Kanfi et al., 2010).

One family of proteins that have been linked to aging and the regulation of CR and the metabolic syndrome are the sirtuins. Sirtuins are highly conserved enzyme homologues of yeast Sir2, with NAD+ dependant deacetylase and / or mono ADPribosyltransferase activity (Imai et al., 2000; Blander & Guarente, 2004; Liszt et al., 2005; Haigis et al., 2006). Studies in several organisms have indicated that sirtuins are critical in the regulation of longevity of Saccharomyces cerevisiae (Kaeberlein et al.,1999), Caenorhabditis elegans (Tissenbaum & Guarente, 2001), and Drosophila melanogaster (Rogina & Helfand, 2004). In addition, mutations in ySir2 or Drosophila Sir2 block the beneficial effect of a CR diet on life span (Lin et al., 2000; Rogina & Helfand, 2004). Thus, in these organisms, sirtuins are pivotal in regulating both longevity and the role of metabolism in life span. With regard to mammalian sirtuins (SIRT1-7), research conducted at the lab of Dr. Chaim Cohen has focused on SIRT6's role in aging. The NAD +-dependent SIRT6 deacetylase is a therapeutic candidate against the emerging metabolic syndrome epidemic. SIRT6, whose deficiency in mice results in premature aging phenotypes and metabolic defects, was implicated in a calorie restriction response that showed an opposite set of phenotypes from the metabolic syndrome (Kanfi et al., 2010). To explore the role of SIRT6 in metabolic stress, wild type and transgenic (TG) mice overexpressing SIRT6 (also called MOSES, Mouse Overexpressing Exogenous Sirt6) were fed a high fat diet. In comparison to their wild-type littermates, SIRT6 TG mice accumulated significantly less visceral fat, LDL-cholesterol, and triglycerides. TG mice displayed enhanced glucose tolerance along with increased glucose-stimulated insulin secretion. Gene expression analysis of adipose tissue revealed that the positive effect of SIRT6 overexpression is associated with down regulation of a selective set of peroxisome proliferator-activated receptor-responsive genes, and genes associated with lipid storage, such as angiopoietin-like protein 4, adipocyte fatty acid-binding protein, and diacylglycerol acyltransferase 1, which were suggested as potential targets for drugs to control metabolic syndrome. These results demonstrate a protective role for SIRT6 against the metabolic consequences of diet-inducedobesity and suggest a potentially beneficial effect of SIRT6 activation on age-related metabolic diseases.

Though it has been shown that the expression of SIRT6 plays a critical role in aging in mice, further research is required to understand the precise mechanism by which it acts. By use of cloning techniques, we intend to target specific tissues with overexpression of SIRT6 in mice to better understand its mechanism. To this end Chaim Cohen's lab is currently developing special transgenic mice using the Cre-Lox method and the TARGATT system recently developed by Stanford University to specifically overexpress SIRT6 in the major metabolic tissues, including WAT, liver, and muscle. By isolating the tissue by which SIRT6 acts, this will help understand the mechanism by which longevity is achieved. Additionally, the liver and WAT are sexually dimorphic tissues, and the longevity effect was only seen in males. Therefore, researching overexpression of SIRT6 in these

tissues will lead to a better understanding of gender-specific effects in SIRT6 TG mice. Estrogen levels and activation via phosphorylated estrogen receptor will be examined in western blot analysis, and by real-time PCR. Once the sirtuin-dependent longevity mechanism is elucidated, this paves the path for small molecule activators of sirtuins for use in treating age-related diseases, particularly diabetes and obesity.

Under the supervision of Shoshana Naiman and Reuven Gil in the Laboratory of Dr. Chaim Cohen of the Life Sciences Department at Bar Ilan University, I aided in the SIRT6 longevity research through various molecular biology techniques. I planned and cloned the SIRT6 gene into a carrier plasmid, which will later be used to transform mouse DNA to over-express SIRT6. This cloning included use of bioinformatics programs to plan the primers, the use of bacteria and PCR machines, and analysis of DNA sequencing. Although this very promising research is still in its early stages, we hope to uncover this precise mechanism of aging, which will undoubtedly prove invaluable in tackling the ever-growing problem of age-related diseases.

References:

Blander G, Guarente L (2004) The Sir2 family of protein deacetylases. Annu. Rev. Biochem. 73, 417–435.

Fontana L, Klein S (2007) Aging, adiposity, and calorie restriction. JAMA 297, 986–994.

Grundy SM, Cleeman JI, Daniels SR, Donato KA, Eckel RH, Franklin BA, Gordon DJ, Krauss RM, Savage PJ, Smith SC Jr, Spertus JA, Costa F (2005) Diagnosis and management of the metabolic syndrome: an American Heart Association / National Heart, Lung, and Blood Institute Scientific Statement. Circulation 112, 2735–2752.

Haigis MC, Mostoslavsky R, Haigis KM, Fahie K, Christodoulou DC, Murphy AJ, Valenzuela DM, Yancopoulos GD, Karow M, Blander G, Wolberger C, Prolla TA, Weindruch R, Alt FW, Guarente L (2006) SIRT4 inhibits glutamate dehydrogenase and opposes the effects of calorie restriction in pancreatic beta cells. Cell 126, 941–954.

Huang PL (2009) A comprehensive definition for metabolic syndrome. Dis. Model Mech. 2, 231–237.

Imai S, Johnson FB, Marciniak RA, McVey M, Park PU, Guarente L (2000) Sir2: an NAD-dependent histone deacetylase that connects chromatin silencing, metabolism, and aging. Cold Spring Harb. Symp. Quant. Biol. 65, 297–302.

Kaeberlein M, McVey M, Guarente L (1999) The SIR2 / 3 / 4 complex and SIR2 alone promote longevity in Saccharomyces cerevisiae by two different mechanisms. Genes Dev. 13, 2570–2580.

Kanfi, Y, Peshti, V, Gil, R, Naiman, S, Nahum, L, Levin, E, Kronfeldschor, N, and Cohen, H (2010) SIRT6 protects against pathological damage caused by diet-induced obesity. Nature 483, 218-221.

Lin SJ, Defossez PA, Guarente L (2000) Requirement of NAD and SIR2 for life-span extension by calorie restriction in Saccharomyces cerevisiae. Science 289, 2126–2128.

Liszt G, Ford E, Kurtev M, Guarente L (2005) Mouse Sir2 homolog SIRT6 is a nuclear ADP-ribosyltransferase. J. Biol. Chem. 280, 21313–21320.

McCay CM, Crowell MF, Maynard LA (1935) The effect of retarded growth upon the length of life span and upon the ultimate body size. J. Nutr. 10, 63–79.

Milionis HJ, Florentin M, Giannopoulos S (2008) Metabolic syndrome and Alzheimer's disease: a link to a vascular hypothesis? CNS Spectr. 13, 606–613.

Rogina B, Helfand SL (2004) Sir2 mediates longevity in the fly through a pathway related to calorie restriction. Proc. Natl Acad. Sci. USA 101, 15998–16003.

Tissenbaum HA, Guarente L (2001) Increased dosage of a sir-2 gene extends lifespan in Caenorhabditis elegans. Nature 410, 227–230.

Weindruch R, Walford RL (1988) The Retardation of Aging and Disease by Dietary Restriction, Springfield, IL, USA: homas.

Avi Bursky-Tammam (YC) and Michaela Gasner (York): "Isolation of a TAX-specific TCR suitable for the generation of a T-cell mediated immune response against HTLV-1"; Professor Cyrille Cohen (Life Sciences).

Human T-cell lymphotrophic virus (HTLV), the first isolated retrovirus, has infected close to twenty million people worldwide. HTLV can cause leukemia, as well as a wide range of inflammatory diseases. One of its antigens, the TAX protein, was shown to be recognized by cytotoxic CD8 T-cells. Nevertheless, as of yet no treatment exists for acute or chronic human HTLV infection.

The immune system is comprised of many different types of cells, most importantly the T-cells, which are responsible for most effector functions in the immune response. Each T-cell expresses a unique receptor, the T-cell receptor (TCR), specific to one particular antigen. A TCR is composed of two chains, alpha and beta, each of which contains a variable and constant region. The variable region is what makes the TCR specific to one unique antigen. Thus, the T-cell can recognize certain antigens expressed by a tumor as part of the immune system's response to defend the body. As such, T-cells can mediate the regression of large tumor burdens in terminally-ill patients.

Yet since the recognition of a tumor is solely based on the interaction of a particular TCR with its cognate antigen on the tumor, and as it is not always possible to isolate such T-cells, adoptive immunotherapy has become a growing area of research. Adoptive immunotherapy involves genetically engineering T-cells to express a defined cancer-specific receptor. In this work, we aimed to isolate a TCR specific for the HTLV-1 virus, which could in turn be used to generate a potent anti-viral response in patients.

In order to isolate the T-cell receptor that recognizes the TAX protein, mice were immunized with the TAX antigen and RNA was then isolated from their T-cells. After reverse transcription, we screened this genetic information for the different TCR alpha and beta chains. Fifty-seven primers were used (thirty-two for alpha and twenty-five for beta) in order to identify the region of DNA that corresponds to the alpha and beta regions. Multiple PCR reactions were performed under specific reaction conditions in order to narrow down the possible alpha and beta subfamilies.

After confirmation by sequencing, we have isolated three families for the alpha chain, namely Va12.1, Va14 and Va16. For the beta chain, the relevant families were Vb12.1, Vb16.1, and

Vb19.1. Furthermore, in order to integrate and express the alpha and beta chains into the genome of T-cells, we initiated the construction of a clinically-approved retroviral vector encoding the TAX-specific TCR.

Further functional experiments will be performed to determine the exact alpha and beta chains that compose the desired T-cell receptor. Overall, the successful completion of this project will yield a novel, highly potent TCR to be employed for the genetic modification of T-cells from HTLV-infected patients, mounting a robust immune response against HTLV-1.

Nathan Japhet (YC): ""Plants' Unique Ecophysiological Adaptations' Effect on the Vertical Distribution of Nematode Populations in Coastal Sand Dunes"; Professor Yossi Steinberger (Life Science).

Coastal sand dune ecosystems are characterized by deposition and erosion processes caused by the wind's movement of sand. Plant cover plays a major role in dune stabilization because it reduces open sand cover and movement; although, plant cover, and its distribution in an uninhabited dune area, is itself influenced by erosion, deposition and environmental stresses like nutrient deficiency, salinity, e.t.c. The different plant species growing on sand dunes therefore play an important role as bio-indicators of a sand dune's relative stability or mobility. In coastal sand dune ecosystems, plants function as "nutrient islands" and moderate the abiotic aspects of their surroundings. Due to the harsh (e.g. nutrient source limitation) xeric environments, development of different ecophysiological adaptations among plants communities generates the formation of distinct microhabitats underneath plant species. The presence of the different microhabitats will be the major force in determining the composition, density and distribution of soil organisms.

One of the most important soil biota groups are nematodes. Soil free-living nematode populations are one of the most numerous groups among multi-cellular animals, are crucial to nutrient cycling and decomposition, and are sensitive to ecosystem disturbances, which lets them be used as indicators for understanding the health and processes of soils.

The goals of the present study were to determine the effect different plants' ecophysiological adaptations had on the vertical distribution of free-living soil nematode populations in coastal sand dunes. Samples were collected in sand dunes near Yavne, Israel in June 2012 from underneath three plants with significantly different ecophysiological adaptations: Echium angustifolium, a perennial flowering shrub thought to have anti-nematode properties; Stipagrostis lanata, a low-lying perennial grass and an indicator of a stable dune system; and Artemisia monosperma, a perennial low sand-fixing shrub and an indicator of a mobile dune system. An inter-plant area was used as a control. Several soil parameters were observed, including soil water content, organic matter, salinity, conductivity, and pH.

The results demonstrated that soil water content (SWC) and pH were significantly different under different plants and inter-plant areas, with the highest values found under Echium angustifolium (pH) and Stipagrostis lanata (SWC). SWC and pH were positively correlated with nematode community density, which was significantly higher under Echium angustifolium than other locations; the lowest density of nematode communities was under Artemisia monosperma and control samples. In previous studies, however, SWC has been shown to negatively correlate with the density of soil nematode communities due to excess water in soil pore caves reducing predator-prey interactions. It seems that SWC is only positively correlated with nematode density in the short term. Nematode density was not significantly different among soil depths in Echium angustifolium (P= 0.96) and Artemisia monosperma (P= 0.95) locations; demonstrating those plants' ecophysiological adaptations effect is more significant than soil depth. Nematode density under Stipagrostis lanata and control locations did vary significantly by depth due to the lack of adequate plant cover of the surface soil layer. The anti-nematode properties of the Echium shrub did not have the expected effect on nematode density and further research is needed into its anti-nematode properties.

Steven (Yosef) Krausz (YC): "Deep Sea Nitrogen Fixation in Oligotrophic Waters"; Professor Ilana Berman Frank (Life Science).

Nitrogen fixation, the process by which organisms use dinitrogen (N_2) as a substrate to produce ammonia, is an important source of nitrogen (N) to nutrient-poor ecosystems. There are significant imbalances in the oceanic fixed-nitrogen budget, as the sink terms in the oceanic fixed-nitrogen budget significantly exceed the current estimates of N_2 fixation and other source terms for fixed nitrogen.

Mohr et al. (2010) argued that the $^{15}N_2$ tracer addition method significantly underestimates N_2 fixation rates when the $^{15}N_2$ tracer is introduced directly to a seawater sample as a gas bubble. The injected $^{15}N_2$ gas bubble does not attain equilibrium with the surrounding water, and therefore leads to a $^{15}N_2$ concentration lower than assumed by the method used to calculate $^{15}N_2$-fixation rates. Mohr therefore proposed a modified $^{15}N_2$ tracer method based on the addition of $^{15}N_2$-enriched seawater. This method provides instantaneous, uniform nitrogen enrichment, and allows more accurate calculations of N_2 fixation rates for both field and laboratory studies.

Our group investigated the potential effect of the addition of $^{15}N_2$-enriched seawater, which dilutes the seawater sample, on selected planktonic communities and rate measurements in the Gulf of Aqaba.

Several research groups world-wide are performing these experiments in various waters representing different geographic locations and trophic environments with varying salinity, composition of organic matter, and diazotroph-community composition.

Our second objective was to investigate the contribution of heterotrophic diazotrophy in the Gulf of Aqaba. Recent evidences from summer 2009, based on bacterial versus primary productivity ratios and N_2 fixation rates done at the aphotic zones (<200 m), suggest the dominance of heterotrophic diazotrophs (compared to autotrophic diazotrophs, mainly Trichodesmium). CTD profiles (including pressure, temperature, salinity, oxygen, and fluorescence), nutrients (including phosphate, silicic acid, nitrite+nitrate,), Chlorophyll a, Flow Cytometry, bacterial production (BP), molecular analyses (DNA and RNA), FIRe, POC/N/P, N_2 fixation (both methods), primary productivity (^{13}C and ^{14}C), and MIMS were measured at various locations and depths in the Gulf of Aqaba.

Experiment was directed by Eyal Rahav of the Ilana Berman-Frank Laboratory

Mohr W, Großkopf T, Wallace DWR, LaRoche J (2010) Methodological Underestimation of Oceanic Nitrogen Fixation Rates. PLoS ONE 5(9): e12583. doi:10.1371/journal.pone.0012583

Montoya JP, Voss M, Ka'hler P, Capone DG (1996) A simple, high-precision, high-sensitivity tracer assay for N2 fixation. Applied Environmental Microbiology 62:986–993.

Aliza Loshinsky (SCW): "The role of the de-ubiquitinase UBP10 in DNA Double Strand Breaks Repair in Saccharomyces Cerevisiae"; Professor Shay Ben-Arroya (Life Science).

By: Aliza Y. Loshinsky[1], Yifat Zuckerman[2], and Shay Ben Aroya[2]
[1]Stern College for Women, Yeshiva University, New York, NY;
[2]Department of Life Sciences, Bar Ilan University, Ramat Gan, Israel

Chromosomal Instability, the loss or gain of large chromosomal segments, leading to aneuploidy or gross chromosomal rearrangement has been discovered in the vast majority of malignancies and tumors. Gross chromosomal rearrangements can be caused by double strand breaks (DSBs) in the DNA that are not repaired.

Evidence has shown that proteasome-mediated degradation is involved in the repair of DSBs. Previously, a screen was carried out in the lab to find the proteins that need to be degraded by the proteasome for a successful completion of the repair process. One of the hits was Ubp10, a deubiquinase that de-ubiquitinates histone H2B. Although Ubp10 was not found to be a target of the proteasome, the overexpression of Ubp10 in media containing DNA damaging agents caused severe growth defects. Previous studies have shown a direct link between the ubiquitilation of histone H2B and the timely and successful repair of DSBs in human cells. The goal of this project is to further understand how the over production of de-ubiquininases, which results in their gain of function, will affects the repair of a specificly induced DSB.The baker yeast Saccharomyces cerevisiae is used as a model system.

A homologous recombination assay was performed using two samples of cells from the MK203 strain, one sample of the wild type cells and one sample of cells that was transformed with a GAL1- UBP10 plasmid. The MK203 strain contains two alleles of the URA3 gene. One allele, on chromosome V, contains a cut site for the galactose-induced HO endonuclease. Thus, transferring the cells to a galactose media induces a single DSB in chromosome V. The cells then use the mechanism of homologous recombination to repair the DSB, using the other allele of the URA3 gene, on chromosome II, as a template for repair. The allele of the URA3 on chromosome II differs slightly from the allele on chromosome V in that it does not have a HO endonuclease cut site and it does contains restriction sites for the restriction enzymes EcoRI and BamHI. Thus, the repaired chromosome will not have an HO cut site and but will include restriction sites for BamHI and EcoRI.

After the yeast cells were induced with a DSB, a sample of cells was taken every 30 minutes. When all the samples were obtained, the region of the DNA were the DSB was induced was amplified. The samples were then treated with the restriction enzyme Bam HI to discover the extent which DNA repair occurred by homologous recombination and gene conversion. The cells that did successfully repair the DSB are expected to show two smaller bands of DNA when run on a gel, compared to the cells that did not undergo DNA repair and gene conversion and are expected to show one large band. If the overexpression of Ubp10 does inhibit timely DSB repair, it is expected that the cells overexpressing Ubp10 will show one large band for more samples, indicating that the cells require a longer period of time to undergo DNA repair and gene conversion. At this time, the results of the study are not yet conclusive.

Sarina Miller (SCW): "Calibration of Primary and Secondary Antibodies for Ideal Immunofluorescence Staining for VZV Research"; Professor Ron Goldstein.

Sarina Miller[1], Anna Sloutskin[2], and Prof. Ronald S. Goldstein[2]

[1]Stern College for Women, Yeshiva University, New York, NY;
[2]Department of Life Sciences, Bar Ilan University, Ramat Gan, Israel

Illnesses caused by human neurotrophic viruses have been difficult to study because of the limited availability of human neurons for experimentation. Human embryonic stem cells (hESC) are pluripotent cells that can be differentiated into neurons, thereby providing a potentially unlimited source of this previously difficult to obtain cell type. Since cultures of differentiating hESC contain many cell types, it is important to be able to identify which cells are neurons. In addition, it is important to know which subtypes of neurons are produced by the differentiation method developed in our lab.[2]

hESC-derived neurons were recently shown to be a useful tool for the study of Varicella Zoster virus (VZV), the cause of Varicella Zoster (chicken pox) and Herpes Zoster (shingles). VZV is a human specific neurotrophic virus that infects peripheral neurons. In order to use these neurons as a model to study VZV, we must confirm that they (as well as other types of cells) were infected with VZV. While antibodies often stain specifically antigens in non-neuronal cells (such as in MeWo and Arpe cells), the same antibodies often react with neurons in a non-specific manner, requiring additional testing.

Indirect immunofluorescence staining is a technique using antibodies to detect specific molecules found in a cell and to thereby identify and characterize its phenotype. Our work involved determining ideal dilutions of primary and secondary antibodies to produce strong staining that is easily visible and has minimal non-specific background staining. Antibodies can be raised against antigens that indicate different stages of neural development or viral infection. Primary antibodies added to cells bind to the antigen, and are detected with a fluorophore-tagged secondary antibody for visualization with a fluorescence microscope.

24-well-plates containing coverslips with various cell lines[3] were fixed with 4% paraformaldehyde when they reached approximately 80% confluence. These coverslips were blocked to prevent non-specific antibody binding, and exposed to primary antibodies at varying dilutions for 1 hour (room temperature) to overnight . The coverslips were subsequently exposed to various[4] dilutions of a secondary antibody for 40 minutes, counterstained with Hoechst (specific to nuclei), mounted on slides, and analyzed using a fluorescence microscope. The dilutions tested ranged from 1:5 to 1:50,000.

Primary antibodies calibrated included antibodies specific for neurofilament-m subunit (polyclonal, 1:1000), E7

specific to microtubules (1:100), Tau specific to axons (polyclonal 1:350, monoclonal 1:100), Brn3a specific to transcription factors in the nuclei of peripheral sensory neurons (polyclonal and monoclonal, 1:250), and a monoclonal IgM antibody specific to actin (1:5). Antibodies to VZV proteins that we calibrated included polyclonal ORF62, ORF63, and ORF4 regulatory proteins, the gE membrane protein (1:10,000), and monoclonal ORF61, ORF62 and ORF63 (1:10,000). The VZV antibodies were kindly provided by Prof. Paul Kinchington (University of Pittsburgh, USA).

Secondary antibodies calibrated included 488 donkey anti mouse (green fluorescence, 1:250), 488 streptavidin (green, 1:1000), Cy2 goat anti mouse (green, 1:500), and Texas red IgM anti mouse (red, 1:100).

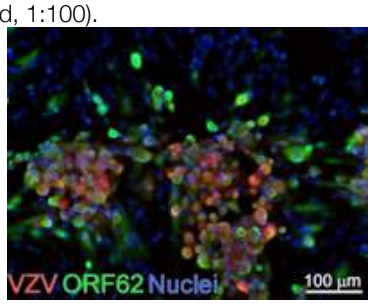

Fig. 1 *MeWo cells infected with VZV expressing ORF66-bound RFP (red) and stained with antibody against ORF62 (green) at a dilution of 1:10,000. Nuclei are stained with Hoechst (blue). The figure shows the specific staining of the ORF62 antibody to the membranes of the infected cells.*

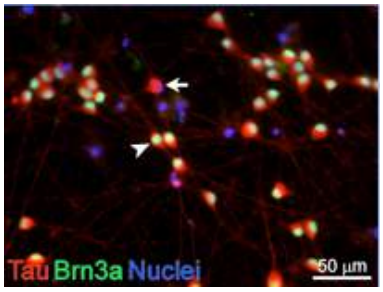

Fig. 2 hESC derived neurons stained with the axonal marker Tau (red) and Brn3a (green) primary antibodies. The nuclei of the neurons are stained with Hoechst (blue). Brn3a detects a transcription factor and can therefore be seen prominently in the nuclei of the cells. The presence of a Brn3a stain indicates that the neuron may be a sensory neuron. The arrow is pointing to a neuron lacking Brn3a, in contrast to the neuron indicated by the arrowhead that was stained by Brn3a.

References:
[1]Pomp O., Brokhman I., Ben-Dor I., Reubinoff B., Goldstein R. S.. 2005.Generation of peripheral sensory and sympathetic neurons and neural crest cells from human embryonic stem cells. Stem Cells 23:923–930.
[2]Cell lines used for experiments included MeWo (human melanoma line), Arpe ARPE-19 (human retinal pigmented epithelial cells), Vero (green monkey kidney epithelial cells), PA6 (mouse stromal cells), and human neurons derived from the H9 cell line.
[3] For most experiments, only one antibody was calibrated, and the other was maintained at a constant previously tested dilution.

Dahlia Pasik (SCW): "Identifying the Aging Gene in Yeast through the Use of a Microfluidic Device"; Professor Doron Gerber (Life Sciences).

By: Dahlia Pasik1, Maria Cher2, Orshay Gabay 2, and Doron Gerber2
[1] Stern College for Women, Yeshiva University, New York, NY;
[2] The Mina & Everard Goodman Faculty of Life Sciences, Bar-Ilan Institute of Nanotechnology & Advanced Materials, Israel

The budding of yeast serves as model organism for research on aging. However, it is difficult to observe the aging pattern in yeast through the classical approach of micromanipulation, as the cells are grown on an agar plate. It is therefore almost impossible to follow the cell and organelle morphologies and track molecular markers throughout the lifespan of individual cells. Additionally, the process is laborious and time-consuming, which makes it difficult to preform large-scale screening for mutants with lifespan phenotypes. Therefore, the development of the microfluidic system has enabled us to track individual mother cells throughout their lifespan, allowing for direct observation of cell-cycle dynamics and various other molecular markers. The microfluidic system is a device which allows the retention of mother yeast cells while at the same time allowing for the discarding of the daughter cells. The mother yeast cells adhere to the device through chemical modification, and they therefore are able to stick to the glass surface of the device. Specifically, Sulfo-NHS-LC-biotin is added to the yeast cells and biotinylated-BSA, followed by neutravidin, is added to the glass surface. Through the formation of the biotin-avidin complex between the mother yeast cells and the device, the mother cells remain on the microfluidic system while the daughter cells are flushed away.

The microfluidic system device is comprised of two layers. The first layer, or the 'flow layer', connects the network of reaction chambers. The second layer, or the 'control layer', controls the flow of the liquid within the reaction chambers. During the experiment, we found that yeast flow is sensitive to the height of the chamber. When using the microfluidic device with a chamber height of 14 µm, the yeast cells aggregated within the inputs. However, when the height of the chamber was enlarged to 25 µm, we successfully obtained a continuous flow of yeast within the microfluidic device (see Figure 1).

The use of a light microscope allowed for observation of a sufficient amount of yeast cells within all of the reaction chambers. We then checked for the immobilization of the mother yeast cells to the device through the biotin-avidin complex. When the yeast was attached to Sulfo-NHS-LC-biotin, it adhered to the avidin that was present on the device. However, yeast aggregates did form when the concentration of 106 yeast cells per ml were used. This can perhaps be attributed to either a high yeast concentration or to the concentration of the NHS attached to the yeast.

The next step will be to optimize the concentration of the NHS bound to the Biotin, supply food for the yeast, and to visualize the budding process of the yeast. Although we currently can only screen yeast sequentially, the long-term goal is to screen a library of yeast in parallel through use of the microfluidic device1.

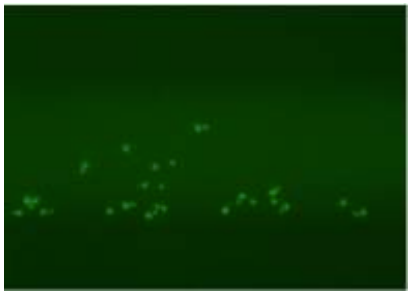

Figure 1: Fluorescent image of GFP-labeled yeast viewed within the microfluidic device

Molecular Phenotyping of Aging in Yeast Cells Using a Novel Microfluidic Device. Zhengwei Xie, et. al. Aging Cell, (2012) 11, pp599-606.

Shira Redlich (UPenn): "Mechanisms of Gene Regulation: Nuclear Speckles and Dbp5"; Professor Yaron Shav-Tal (Life Sciences). *

After transcription in the nucleus, the pre-mRNAs undergo several processes before they are released for translation in the cytoplasm. These processes include capping, splicing, and polyadenylation. Many details of this process are still unknown and are currently being studied in scientific research

Professor Yaron Shav Tal's lab is exploring various aspects of the gene expression pathway, both its mechanisms and dynamics. Members of the lab specifically focus on nuclear speckles (Figure 1), clusters of mRNA splicing and transcription factors found inside the nucleoplasm. Many properties of the speckles are still unknown such as how the splicing factors organize themselves into clusters with no membrane and how exactly the dynamics of the speckles relate to transcription and processing. To investigate the properties of these speckles, they have been using the Clk1 enzyme, which has been found to phosphorylate these splicing factors, allowing them to subsequently be released into the cytoplasm.

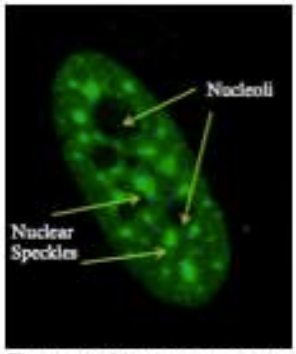

Figure 1: Nuclear speckles

In a previous experiment, a double transfection was performed with Clk1 and Cherry. The Cherry is used so that the cells that took in the plasmids can be recognized using immune-fluorescent microscopy. While the double transfection proved to be successful, performing a single transfection with a plasmid with the two genes fused together would be more efficient and result in more successful transfections. As a result, I have cloned a plasmid to contain both the Clk1 and RFP (Red Fluorescent Protein) genes (Figure 2) so that a double transfection is no longer necessary. This project included various techniques including Polymerase Chain Reaction (PCR), gel electrophoresis, DNA cloning, bacterial transformation, DNA mini-prep, DNA gel extraction, and immuno-fluorescent microscopy.

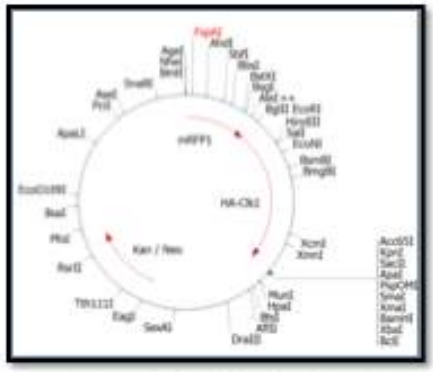

Figure 2: RFP-HA-Clk1 Plasmid

After the the vector and insert were digested with the enzymes BglII and Kpn1 and then ligated, the length of the plasmid was verified using gel electrophoresis and extracted through a DNA purification process. Then a bacterial transformation was performed using a Kanamycin medium, as the original vector contained kanamycin resistance. The surviving colonies were then picked and extracted from the bacteria through a mini prep process and then transfected into U20S cells which already had a specific splicing protein tagged with GFP (Green Fluorescent Protein). We examined the cells under fluorescent microscopy and observed that all of the cells that took in the plasmid (as seen by the red color), did not contain speckles; rather, the speckles were disassembled and the tagged splicing factors were scattered throughout the nucleoplasm (Figure 3).

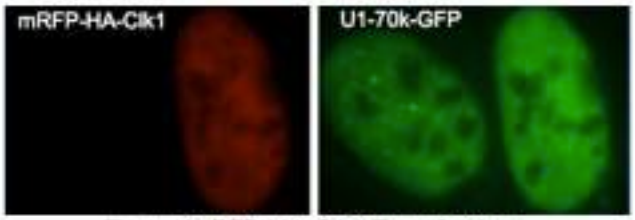

Figure 3: RFP-HA-Clk1 Transfection

In another project, members of Professor Shav Tal's lab have been exploring mRNA dynamics and specifically mRNA export out of the nucleus. They are currently building on previous research that has indicated the importance of the protein Dbp5 in this process. We have transfected U20S cells with a mutant Dbp5 gene, producing a mutant Dbp5 protein tagged with CFP (Cyan Fluorescent Protein), as indicated by the light blue color. In these cells, the mRNA was already tagged with RFP-MS2, as seen by the red color. When compared to the control cells under FISH microscopy, we found that, there is an abundance of mRNA "stuck" in the nucleus of the mutant cells (Figure 4). This further suggests that Dbp5 plays an essential role in mRNA export from the nucleus. Future

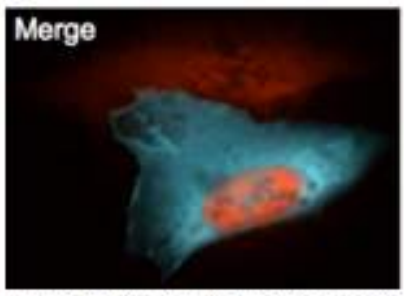

Figure 4: Mutant Dbp-5 Transfection

exploration of the mechanism of splicing factors in nuclear speckles and the specific role of Dbp5 will allow Professor Shav Tal's lab to learn more about specific gene regulation processes.

**Under the supervision of Noa Neufeld and Rakefet Ben Yishai*

Figure 1: N. Neufeld; Figure 3: N. Neufeld, Figure 4: R. Ben Yishai

Mordechai Smith (YC): "The establishment of trnsgenic fish that express synaptic markers on MCT8-positive cells"; Professor Lior Appelbaum (Life Sciences).

Allen-Herndon-Dudley syndrome (AHDS) is an X-linked psychomotor retardation that is characterized by hypotonia (low muscle tone), muscle hypoplasia (low number of muscle cells), paroxysmal dyskinesia (sudden episodes of abnormal involuntary movements), and severe cognitive impairment. AHDS symptoms also include abnormal levels of thyroid hormone (TH), specifically, high serum T3 levels and low serum T4 levels. AHDS is associated with mutations in the trans-membrane transporter protein monocarboxylate transporter 8 (MCT8).

In this project we used the zebrafish (Danio rerio) model to visualize MCT8 expression cells with fluorescent markers. The zebrafish is a powerful vertebrate model with conserved organization of the central nervous system (CNS). The Mct8 gene is highly conserved in zebrafish with its mammalian ortholog (shares 56-57% homology).

Dr. Appelbaum's lab is seeking to understand the neurological mechanism underlying AHDS. Because neurological impairment in AHDS is rooted in MCT8 deficiency, we wanted to check synaptic activity, as loss of MCT8 may affect synaptogenesis and synaptic plasticity and ultimately affect neuron function. In order to do so, DNA constructs containing mct8 promoters that drive the expression of the coding sequences of either the presynaptic protein SYP or the post-synaptic proteins PSD95 and GPHN fused to EGFP (green fluorescence) or tagRFP (red fluorescence), were injected into one-cell-stage-embryos. These embryos (F0) were raised to adulthood and, in this project, F0 fish were screened to isolate stable transgenic lines.

To find a transgenic fish, we must first assure that the F0 fish has incorporated the transgene into its germline cells. Germline cells are progenitors to gametes such as eggs and sperm. Only if a F0 fish has incorporated the new gene into its germline will its progeny have the modified gene.

My project was to screen all F0 fish for the presence of several transgenes in the germline. Screening is done in two steps. First, I outcrossed all F0 transgenic fish with wild type fish. I then purified DNA from the ensuing batch of embryos (F1). From the DNA, I amplified the region of the transgene (EGFP or tagRFP) using Polymerase Chain Reaction (PCR). The resulting product was run through a gel electrophoresis which allowed me to screen for the presence of the transgene. If the F1 DNA contained the transgene, I was able to ascertain that the F0 fish had incorporated the transgene into its germline. The second step in screening required re-crossing the positive F0 fish and observing the F1 for actual fluorescence. A fluorescent binocular was used to observe the fish and any fish that showed positive signs of the fusion protein was considered a line.

I outcrossed 23 mct8:GPHN-tRFP fish, 16 mct8:PSD95-EGFP fish, and 4 mct8:SYP-EGFP fish. I received a positive PCR result in 3 mct8:PSD95-EGFP fish, 3 mct8:GHPN-tRFP fish, and 2 mct8:SYP-EGFP fish. Of those fish, two mct8:PSD95-EGFP fish have shown fluorescence and may be raised for further analysis of MCT8 function. These lines may also shed light on the neurological mechanism of AHDS.

Miriam Steinberger (SCW): "Regulation of the adaptor protein LAT in Natural Killer immune cells"; Professor Mira Barda Saad (Life Science).

Miriam Steinberger, Omri Matalon, Marina Piterburg and Mira Barda-Saad
Bar Ilan University, Remat Gan, Israel

Natural killer (NK) cells are innate immune cells that have highly specific target cell recognition mechanisms which cause secretion of cytokines and trigger target cell cytotoxicity. NK cells are activated without prior exposure to antigens and rather depend on germline-encoded receptors for their activation. They play an important role in early protection against viral infections, prevention of tumor proliferation and development of autoimmunity. However, the exact mechanisms of how NK cells are positively and negatively regulated remain unknown.

LAT is a scaffold protein which binds to and thus transports activating proteins toward the cell synapse, serving as a linker between activating receptor engagement and downstream signaling cascades. LAT is known to be crucial for the activation, and thus for the function, of both T and NK-cells as knockout of LAT render the cells hypo responsive. In addition, LAT was shown to undergo ubiquitylation dependent degradation upon T cell activation, which facilitates in the attenuation of T cell function, thereby preventing the development of autoimmune disorders. However, while the mechanisms that negatively regulate LAT in T cells were thoroughly investigated, those mechanisms in NK cells, and their effect on NK cell function, are yet to be characterized. Thus, in this study we focused on the investigation of LAT negative regulation. We found, using a combination of molecular biology and biochemical approaches, that upon NK cell interaction with target cells LAT is down regulated.

Acknowledgements
Bar Ilan Summer Research Program, Dr. Mira Barda-Saad, Omri Matalon and Marina Piterburg.

PSYCHOLOGY, BRAIN, & CLINICAL NEUROPSYCHOLOGY

Menachem Benzaquen (U Ottawa): "*Aplysia* Feeding Behaviors"; Professor Avi Susswein (Life Science/Brain).

When one hears the term "model organism," rarely does the sea hare *Aplysia* come to mind. These gastropods, however, have been chosen by neuroscientists around the world as a model for studying neurobiology due to their relatively simple nervous systems.

Professor Avraham Susswein's lab studies the feeding behaviors of *Aplysia*. Experiments were conducted to investigate how the unconventional neurotransmitter Nitric Oxide (NO) and sex pheromones affected *Aplysia* feeding behaviours. NO is considered an unconventional neurotransmitter because it is a gas and additionally exceptional because it is a radical one. From previous research, NO had been found to inhibit feeding in *Aplysia*. The sex pheromones on the other hand, which were secreted by mating conspecifics, had been found to increase feeding in *Aplysia*. Our goal was to investigate how NO and pheromones affected *Aplysia* feeding behaviors in tandem. Unfortunately, these experiments did not confirm our hypotheses, and we were left disappointed. Nevertheless, towards the end of the summer, other experiments were carried out to investigate the excitatory and inhibitory effects of food odors in the *Aplysia*'s surrounding environment. The experiments produced better results, and we discovered that food odors in the *Aplysia*'s environment were excitatory when they were present for 1 hour or less. When they were present for more than 1 hour, however, *Aplysia* feeding was inhibited. Our data indicated this because animals that were exposed for 1 hour to food odor consumed more initially than animals exposed longer than 1 hour (whether it be anywhere between 2 to 24 hours). By the conclusion of the experiment, all animals, regardless of time of exposure, had similar eating rates. Further experimentation is needed in the future, however, to draw fully conclusive evidence.

Methods of experimentation used in our lab were relatively simple. Before the experiments, all animals were weighed. Based on their respective weights, food (green algae) was then prepared. Due to the water-absorbent nature of the green algae, all food had to be dried manually before feeding the *Aplysia*. Additionally, the algae had to be dried yet again after being removed from the water at the conclusion of the experiment. Observations of each animal were recorded every five minutes for a period of six hours, thus requiring someone to remain in close proximity for this period of time.

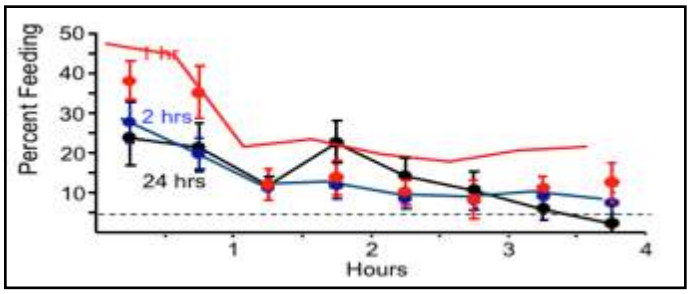

Graph 1. Aplysia feeding as a function of hours exposed to food odor. Graph indicates that when exposed to 1 hour, Aplysia feeding increased.

Koral Dadon (SCW): "Do married couples match on the Wisconsin Card Sorting Test?"; Professor Joseph Glicksohn (Clinical Neuropsychology).

Koral Dadon[1], Hilla Golan-Smooha[2], Revital Naor-Ziv[2] and Joseph Glicksohn[2]
[1]Stern College for Women, Yeshiva University NY, NY
[2]Department of Criminology, and The Leslie and Susan Gonda Multidisciplinary Brain Research Center, Bar-Ilan University, Ramat-Gan, Israel

The Wisconsin Card Sorting Test is a clinical neuropsychological assessment instrument that is used as a means of testing executive or frontal lobe functioning. [1]

The objective of our lab was to utilize a fine grain way of analyzing the performance of a normal population of married couples with the Wisconsin Card Sorting Test (WCST) by closely reading the WCST Manual in order to find whether there was a similarity between couples on perseverative error scores. The participants of the study included thirty-one married couples, part of a larger sample, selected randomly with normal intact families. The research was carried out at the couples' homes where the couples answered the computerized version of the WCST along with other 'pencil and paper' cognitive tasks.

Using the Wisconsin Card Sorting Test Manual, the participant responses are scored based on three dimensions: Correct-Incorrect, Ambiguous-Unambiguous, and Perseverative-Nonperseverative. Responses that match the sorting principle in effect are scored as correct, while incorrect responses are scored as errors. When the client matches a response card to a stimulus card based on only one stimulus characteristic, the principle that is used is obvious and unambiguous to the examiner. For example, a response card with three green circles is matched to the stimulus card with two green stars, which indicates that color is the stimulus characteristic. Additionally, any response that matches a stimulus card on two or more stimulus characteristics such as Color and Form is scored as an ambiguous response. Furthermore, a client that continues to respond to a stimulus characteristic that is incorrect, the response matches the "perseverated-to" principle and is scored as perseverative. Responses that do not match the perseverated-to principle are nonperseverative. [2]

There are three situations that define the perseverated-to principle for scoring perseverative responses. Initially, the first unambiguous error the client makes at the beginning of the test establishes the perseverated-to principle, but is not scored as perseverative. Any subsequent unambiguous error that matches the perseverated-to principle is scored as an "unambiguous perseverative error". Also, an ambiguous response whether it is correct or incorrect can be scored as perseverative when it matches the perseverated-to principle that is currently in effect and is sandwiched between a preceding and following unambiguous responses. Secondly, all responses between the two unambiguous perseverative errors must match the perseverated-to principle in effect for an ambiguous response to be scored as perseverative error or perseverative response. Finally, when the client makes three unambiguous errors to a sorting principle that is incorrect and all responses between the first and the third unambiguous error match this sorting principle, this sorting principle becomes the new perseverated-to principle. However, scoring based on this new perseverated-to principle begins with the second unambiguous error. [2]

Wisconsin Card Sorting Test:

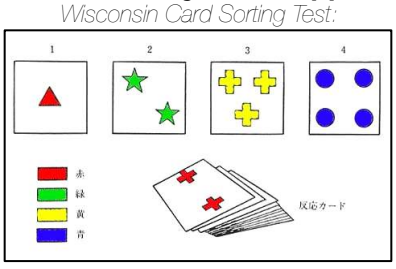

The total number of perseverative errors of the husbands and wives were calculated and plotted on a Scatter Plot. Using SPSS Software, a correlation of 0.436 was obtained, indicating that married couples' perseverative error scores match. This finding supported similarity or assortative mating between married couples.

Descriptive Statistics

	HUSBAND KORAL PER ERROR	HUSBAND KORAL PRE CORRECT	WIFE KORAL PER ERROR	WIFE KORAL PRE CORRECT	Valid N (listwise)
N	31	31	33	33	31
Minimum	7.00	.00	6.00	.00	
Maximum	42.00	10.00	63.00	15.00	
Mean	17.6452	2.1935	21.3636	2.7273	
Std. Deviation	10.11121	2.68849	13.79723	3.78544	

Paired Samples Correlations

		N	Correlation	Sig.
Pair 1	HUSBAND KORAL PER ERROR & WIFE KORAL PER ERROR	31	.436	.014
Pair 2	HUSBAND KORAL PRE CORRECT & WIFE KORAL PRE CORRECT	31	.321	.078
Pair 3	HUSBAND PERSERVATIVE RESPONSE & W_K_PERRSER_RESPONSE	31	.436	.014

With regards to perseverative responses, although women scored a little higher than men on perseverative responses, no significant differences between husbands and wives were observed.

Paired Samples Test

		Paired Differences					t	df	Sig. (2-tailed)
		Mean	Std. Deviation	Std. Error Mean	95% Confidence Interval of the Difference				
					Lower	Upper			
Pair 1	HUSBAND KORAL PER ERROR - WIFE KORAL PER ERROR	-4.32258	13.23225	2.37658	-9.17621	.53105	-1.819	30	.079
Pair 2	HUSBAND KORAL PRE CORRECT - WIFE KORAL PRE CORRECT	-.70968	3.91743	.70359	-2.14660	.72725	-1.009	30	.321
Pair 3	HUSBAND PERSERVATIVE RESPONSE - W_K_PERRSER_RESPONSE	-5.03226	16.17505	2.90512	-10.96531	.90080	-1.732	30	.094

References:

[1]. Stano, J. (2002). Wisconsin Card Sorting Test. Rehabilitation Counseling Bulletin, 45(4), 250-251.
[2] Heaton, Robert K. Wisconsin Card Sorting Test Manual: Revised and Expanded. [S.l.]: Psychological Assessment Resources, 1993. Print.

Noam Grysman (York) and Ruth Shach (York): "What do SAD eyes see? "; Professor Eva Gilboa-Schechtman (Psychology).

Social anxiety, also known as social phobia, is a common mental disorder which afflicts approximately 12% of the population. Cognitive-behavioral models of social anxiety dictate that socially-anxious individuals have cognitive vulnerability to social anxiety due to negative information processing biases. Socially anxious (SA) individuals interpret social situations based on dysfunctional assumptions, which result in perceived social danger and anxiety. They selectively attend to negative information about themselves and use this information to make negative self-evaluations and negative predictions about their future social performances. This is known as attentional bias. There are three stages to the acquisition and maintenance of this bias: (1) Vigilance to stimuli perceived as threatening, (2) difficulty disengaging from the stimuli, and (3) once disengaged, avoidance of the stimuli. Eye contact, crucial to social interaction, is often used as a measure of attentional bias in social anxiety. Our study examines the differing visual scan paths of human faces by SA and non-SA people. SA individuals are predicted to (1) engage in eye contact faster than non-SA individuals (vigilance) and (2) break and avoid eye contact after the initial vigilance period (avoidance). In our study, participants free-viewed a set of both male and female faces exhibiting disgusted, sad, happy, angry and neutral expressions (Fig 1), while their visual scan paths were recorded with an eye tracker and analyzed by a new software developed by our lab. Thus far, the results of the experiment are in the processing stages. This study will contribute to clinical research and will have practical applications pertaining to attentional bias modification (ABM), an attentional retraining of automatic attentional biases that have been observed in SA individuals.

Fig. 1

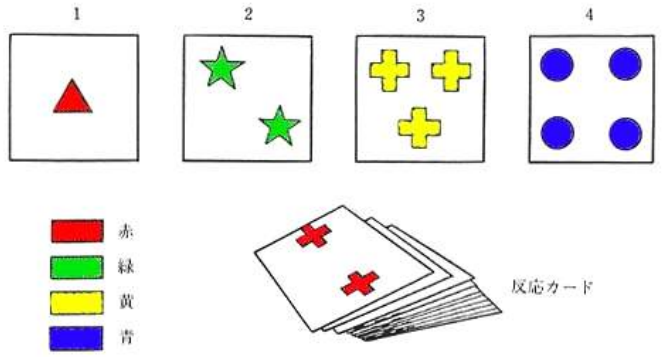

Elianna Kaplowitz (Barnard) and Dani Mandel (YC): "Attention and Distractibility in ADHD and non-ADHD Adults"; Professor Ronny Geva (Brain).

Focused attention has been known to play an integral role in the cognitive learning processes of infants and children. This type of concentrated attention is characterized by an intent facial expression, minimal extraneous bodily activity, a posture enclosing the object of interest and bringing it closer to the eyes, and no talking or soft talking clearly directed to the self. In contrast, inattention and less concentrated types of attention are characterized by a less intent looking at the object, increased extraneous bodily movement, and increased talking (Ruff and Capozzoli, 2003).

While past research has studied focused attention's role in learning and distraction resistance in children (Tellinghuisen and Oakes, 1997; Ruff and Capozzoli, 2003), few such studies have been conducted on adults. The current study sought to determine the role and characteristics of focused attention in the cognitive

learning processes of adults by studying participants with Attention Deficit Hyperactivity Disorder (ADHD) and control participants without ADHD. Individuals with a diagnosis of ADHD are known to exhibit hyperactivity, impulsivity, and most importantly for our study, inattention. Based on this knowledge, we hypothesized that adults with ADHD would display quantitatively less overall focused attention, oscillate more frequently between focused attention and inattention, and be more easily distractible than adults without ADHD.

We tested this hypothesis by observing adults (18+ years of age, N=27) in a structured play setting in which they were presented with one of four puzzle games (picture cards, K'nex, tower puzzle, ball and string puzzle) together with one of four distractor conditions (no experimental distractor, auditory distractor only, visual distractor only, auditory-visual distractor). Each distractor was displayed on a computer monitor positioned at eye level approximately 45° from the subject's line of sight. Recorded videos from each experimental trial were coded by two reliable observers (reliability > 80%) to determine the total duration and number of instances of focused attention and inattention for each game, as well the number of instances of distraction for each distractor condition.

The compiled data was analyzed using SPSS software comparing the ADHD and non-ADHD groups. Several T-tests were conducted using total duration of focused attention and inattention, number of instances of focused attention and inattention, and number of instances of distraction as dependent measures. While we only found a significant effect in latency to focused attention during the picture cards game ($p=0.035$), the total duration of focused attention and total duration of inattention during the picture cards game variables approached significance ($p=0.080$ and $p=0.059$, respectively). This supports the hypothesis that adults with ADHD may display quantitatively less overall focused attention, a finding consistent with previous data on ADHD individuals. Further research should be conducted to explore this apparent trend by testing the generality of this finding as well as by searching for other significant interactions between the experimental variables.

Harris Nickowitz (USC): "Magnetic Stimulation of Rat Brain Neurons"; Professor Alon Korngreen (Brain).

Neurophysiology is the study of nervous system function. Patch-clamp recording, created in the late 1970s, is a major tool in studying the nervous system concerning electrophysiology. Unlike the clamp technique designed to control and measure the electrical properties of large diameter neurons, the patch-clamp technique enables the recording of electrical properties of small-diameter neurons by patching the cell membrane using a glass pipette containing a conducting solution. The pipette is mounted on a stimulating electrode linked to the patch-clamp amplifier. The pipette is visually guided to the cell membrane, and a seal between the two is attempted, using slight negative pressure and depolarization of the membrane. When the current resistance of this seal is in the order of 1-3 GΩ, the current leaking at the interface between the pipette and membrane is smaller than 10 pA. In this state, the whole cell configuration is achieved through breaking the cell membrane by creating a vacuum inside the patch-pipette while in the cell-attached configuration. This creates a continuous medium between the pipette solution and the cytoplasm allowing for cell-wide ionic currents to be recorded.

Transcranial magnetic stimulation (TMS), a non-invasive method for studying the human brain, has potential for use in clinical neurology. This method actively stimulates the brain through the use of a magnetic coil which generates a momentary electromagnetic field. The magnetic coil is placed above the skull over the region of interest, and, consistent with Faraday's law, it induces an electrical field in the brain that can stimulate cortical neurons (Walsh and Rushworth 1999), causing action potentials to occur. TMS differs from other noninvasive methods as it interferes with behavior, making it a powerful tool for investigating the relation between human behavior and brain activity.

Dr. Alon Kongreen's lab constructed an electrophysiological system in order to study the effects of magnetic stimulation on acute rat brain slices, through use of the patch-clamp technique. In this system, both the magnetic threshold (the voltage needed to magnetically stimulate a neuron) and the current threshold (the amount of current needed to stimulate a neuron) were measured. The slices were then preserved, and placed on microscope slides. Using a camera-mounted microscope, the cell bodies were measured and the cells were outlined through a tracing and mapping software, Neurolucida. These tracings were used to create digital neuronal reconstructions. When complete, the reconstructions would then be run through a computer program to recreate neuronal current flow and test the results gathered in vitro.

Through the use of the electrophysiological system and the Neurolucida reconstructions completed thus far, two major conclusions were observed regarding the magnetic threshold of cells. Firstly, the magnetic threshold increases as a function of current threshold, expressing their direct proportionality. Secondly, the magnetic threshold decreases as soma size increases. These results can be of great significance for understanding the basic mechanisms underlying diseases, such as Multiple Sclerosis.